genes

MDPI

Article

Comparative Transcriptomics and Co-Expression Networks Reveal Tissue- and Genotype-Specific Responses of *qDTYs* to Reproductive-Stage Drought Stress in Rice (*Oryza sativa* L.)

Jeshurun Asher Tarun [1,2], Ramil Mauleon [3], Juan David Arbelaez [1], Sheryl Catausan [2], Shalabh Dixit [2], Arvind Kumar [2], Patrick Brown [4], Ajay Kohli [2] and Tobias Kretzschmar [3,*]

1 Department of Crop Sciences, College of Agricultural, Consumer & Environmental Sciences, University of Illinois at Urbana-Champaign, Champaign, IL 61820, USA; tarun2@illinois.edu (J.A.T.); arbelaez@illinois.edu (J.D.A.)
2 International Rice Research Institute, Los Baños, Laguna 4031, Philippines; s.catausan@irri.org (S.C.); s.dixit@irri.org (S.D.); a.kumar@irri.org (A.K.); A.Kohli@irri.org (A.K.)
3 Southern Cross Plant Science, Southern Cross University, Military Rd, East Lismore NSW 2480, Australia; ramil.mauleon@scu.edu.au
4 Department of Plant Sciences, University of California Davis, One Shields Avenue, Davis, CA 95616, USA; pjbrown@ucdavis.edu
* Correspondence: tobias.kretzschmar@scu.edu.au; Tel.: +61-2-6626-3406

Received: 14 August 2020; Accepted: 22 September 2020; Published: 24 September 2020

Abstract: Rice (*Oryza sativa* L.) is more sensitive to drought stress than other cereals. To dissect molecular mechanisms underlying drought-tolerant yield in rice, we applied differential expression and co-expression network approaches to transcriptomes from flag-leaf and emerging panicle tissues of a drought-tolerant yield introgression line, DTY-IL, and the recurrent parent Swarna, under moderate reproductive-stage drought stress. Protein turnover and efficient reactive oxygen species scavenging were found to be the driving factors in both tissues. In the flag-leaf, the responses further included maintenance of photosynthesis and cell wall reorganization, while in the panicle biosynthesis of secondary metabolites was found to play additional roles. Hub genes of importance in differential drought responses included an expansin in the flag-leaf and two peroxidases in the panicle. Overlaying differential expression data with allelic variation in DTY-IL quantitative trait loci allowed for the prioritization of candidate genes. They included a differentially regulated auxin-responsive protein, with DTY-IL-specific amino acid changes in conserved domains, as well as a protein kinase with a DTY-IL-specific frameshift in the C-terminal region. The approach highlights how the integration of differential expression and allelic variation can aid in the discovery of mechanism and putative causal contribution underlying quantitative trait loci for drought-tolerant yield.

Keywords: co-expression network; drought-tolerant-yield; reproductive-stage drought; *qDTY*s; rice; transcriptomics

1. Introduction

Rice (*Oryza sativa* L.) is a staple crop feeding over half of the global population [1]. The Green Revolution accelerated the productivity of rice cultivation across Asia by focusing on irrigated, high input systems [2]. Intensification and expansion into new suboptimal cultivation areas, coupled with changing climatic conditions, however, necessitate a shift towards low input systems. Under resource- and water-limiting conditions, tolerance of both abiotic and biotic stress factors is crucial to ensure productivity.

Traditionally, rice was grown in areas naturally irrigated by seasonal floods [3]. Pre-domesticated rice is essentially a wetland species, making rice more sensitive to drought stress than most other staple crops [4]. Particularly, during the reproductive stage, drought typically causes yield reduction of 50% or more [5–10]. Consequently, water limitation is a major environmental constraint to rice production [11].

Successful strategies to identify factors contributing to drought tolerance involved mapping of quantitative trait loci (QTLs) for grain yield under drought conditions, so-called DTY (drought tolerant yield) QTLs [12]. By crossing the drought-tolerant donor N22 with Swarna, several major-effect DTY QTL, among them *qDTY1.1*, and *qDTY3.2* were identified as having consistent effects on grain yield under reproductive-stage drought stress (RDS) and no apparent yield or performance penalty under non-stress conditions [7]. These were subsequently introgressed into drought susceptible elite parents through backcrossing [13], resulting in the release of several drought-tolerant rice varieties. For example, "Bahuguni dhan-1", a sister line of DTY-IL used in this study, was recently released in Nepal [13]. In addition, several other large-effect DTY QTLs were identified from other populations and utilized for their potential to confer drought tolerance [14–17]. Gene discovery work in *qDTY12.1* resulted in the identification of a NAM transcription factor as an intra-QTL hub gene [18,19].

To unravel specific drought responses in rice, transcriptome studies across different cultivars and drought stress conditions identified hundreds of differentially expressed genes (DEGs) in an organ- and time-specific fashion [1,10,20–27]. Collectively these studies pinpointed key transcription factors (TFs) involved in ABA-dependent and ABA-independent pathways to be upregulated during water deficit stress, effecting osmolyte production, reactive oxygen species (ROS) scavenging and ion transportation [10,22,28].

After an initial focus on studying drought during vegetative stages, the importance of RDS was soon realized [8,23,29–33]. From an applied perspective, grain yield under drought is the key trait, making yield-associated developmental processes and responses under RDS a focus of drought research in rice [8]. Knowledge of broad level biological mechanisms governing RDS responses, however, is still limited [34]. Convincing concepts on how drought-stress-related genes are regulated are still in their infancy. DEG analysis, based on single-genes, often failed to result in meaningful biological interpretations [35,36], prompting the development of network-based techniques that consider complex relationships among genes [37,38].

Gene co-expression networks (GCNs) are increasingly employed to explore system-level functionality of genes and have been found useful for describing the pairwise relationships among genes [39]. GCNs provide a structured pathway for extracting modular responses from large datasets that are often missed by DEG or ANOVA approaches [40]. It shifts the focus from single candidate genes to groups of related genes that likely operate together within a tissue or in response to a stimulus [41]. Genes clustering in a module, provide insight into potential regulatory functions [40,42,43]. An essential application of GCN analysis is to identify functional gene modules, which are a group of nodes that have high topological overlap [44]. Weighted gene correlation network analysis (WGCNA) can be used for co-expression network analysis of gene expression data to find modules of highly correlated genes [45]. In rice GCN analysis provided some insights into gene regulation under drought stress, including (i) consensus modules of downregulated and upregulated genes [46]; (ii) a module enriched for genes involved in water homeostasis and embryonic development, including a heat shock TF [47] and (iii) new candidates involved in drought response [48].

While a number of major QTL for DTY have been discovered, knowledge regarding the underlying physiological mechanisms is largely lacking. On the other hand, while a number of transcriptome studies provided some general insights into drought responses of rice, they did not take presence of specific DTY QTL into account. In the 2014 and 2015 drought field trials at the International Rice Research Institute (IRRI), a DTY introgression line (DTY-IL) performed well under drought without showing a penalty under irrigated conditions. We decided to investigate this line further in a comparative transcriptomic approach against its drought susceptible recurrent parent Swarna.

Our rationale for this study was that combining a functional genomics with a classical genetics approach would improve resolution on drought tolerance mechanisms. By applying a gene co-expression network analysis and focusing on key source (flag-leaf) and sink (emerging panicle) tissues at reproductive stages, which had previously been demonstrated as critical for drought response [43], we speculated that adaptive mechanisms that drive yield under drought could be captured. By comparing the differential expression responses and overlaying genetic variation within the introgressed DTY QTL we further aimed to demonstrate that the differences at the genome-wide transcriptome level are modulated by the introgression segments. Our results support previous findings in respect to general mechanisms underlying drought response, and in addition suggest specific mechanisms underpinning DTY QTL.

2. Materials and Methods

2.1. Plant Materials and Experimental Treatments

Rice genotypes used in this study were: Swarna, a South Asian *indica* mega variety, susceptible to drought stress, and DTY-IL (designation IR 96321-1447-165-B-3-1-2), a highly drought-tolerant F_7 introgression line containing N22 fragments in a Swarna background. DTY-IL is sister line of IR 96321-1447-651-B1-1-2, which was recently released as a drought-tolerant variety in Nepal [13].

Field experiments were conducted in the 2014 and 2015 dry season (DS), and were laid out in an augmented RCB design. The 2014 trial had 420 entries and 6 checks with 5 blocks in a single row per plot while the 2015 trial, had 46 entries and 2 checks with 4 blocks in four rows per plot. For both trials, only checks were repeated based on the number of blocks. For the drought screening, water was removed from the field around 28–30 days after transplanting by opening all drainage canals around the field. PVC pipes measuring 1.1 to 1.2-m long were installed in different parts of the field for water table measurements. The PVC pipes were placed 1 m below the soil surface. The water table was measured regularly starting 1 day after draining the field.

A pot experiment was arranged in a randomized complete block design with two treatments (well-watered and 2-weeks drought-stressed), two genotypes, and six replications in a greenhouse at the International Rice Research Institute (Los Baños, Philippines) from July to November 2015. Three pre-germinated seeds of the two genotypes were initially seeded on white porcelain pots filled with 15 kg of clean puddled field soil (not sterilized). Upon seedling establishment, a healthy seedling was retained in each pot and grown under a well-watered condition in the greenhouse until the booting stage before initiating a dry-down experiment. A day before imposing stress, all the pots were saturated with water and allowed to drain excess water for 24 h to maintain the field capacity (FC) so that the soil moisture amount in each pot was uniform. Then each pot was weighed to know the amount of water at FC. The temperature inside the greenhouse during the stress induction was at a maximum of 30–34 °C and a minimum of 23–26 °C, and a day-time relative humidity of 69%–95% (Figure S1A). During the drought stress period, the pots were weighed daily, and the difference in weight on subsequent days was corrected by adding water to maintain the required FC [49]. For RDS, water was withheld at the reproductive R2 stage, on discrete morphological criteria as described by [50], until the soil moisture level dropped to 75% FC and was maintained for nine days, whereas control plants were well-watered. At day 10, FC was reduced to 50% for three more days (Figure S1B). Flag-leaf and whole panicle samples of well-watered and drought-stressed treatments were collected at the R3 stage [50] on the 12th day of RDS and immediately flash-frozen in liquid nitrogen. Four independent biological replicates for each tissue and each genotype sample were harvested.

2.2. RNA Extraction and Sequencing

Total RNA was extracted using the Qiagen RNeasy Plant Mini Kit (Qiagen, Limburg, The Netherlands). RNA concentration was quantified using Nanodrop spectrophotometer (ND-1000; Nanodrop Technologies, Wilmington, DE, USA), while purity and integrity were established using an

Agilent 2100 BioAnalyzer RNA 6000 Kit (Agilent Technologies, Santa Clara, CA, USA), with a RIN value of 8 used as quality threshold. Illumina library preparation and sequencing were completed following the standard protocols of Macrogen Inc. (Seoul, South Korea). Using Illumina HiSeq 2000 and HiSeq 4000 (Illumina, Inc., San Diego, CA, USA) platforms for the whole panicle and flag-leaf tissues, respectively, 101 bp aired-end sequencing was done. A quality check of raw RNA-Seq reads was performed using FastQC software (version 0.11.5) [51]. The sequencing data have been deposited in NCBI's Gene Expression Omnibus (GEO) database under the accession number GSE145870.

2.3. Transcriptome Assembly and Expression Level Quantification

Raw fastq reads were filtered using Trimmomatic software, version 0.36 [52] using default settings. An indexed transcriptome fasta file was built from the rice japonica genome (IRGSP1.0) and annotation gff3 file from Rice Genome Annotation release 7 (RGAP 7, http://rice.plantbiology.msu.edu/), using the "gffread" function of Cufflinks (version 2.2.1) [53], and Salmon (version 0.7.2) [54] "index" function. Salmon then quantified transcript abundance in quasi-mapping mode directly using the indexed transcriptome and the trimmed high-quality paired-end reads with parameters "-l A, -seqBias and -gcBias" to allow automatic inference of library type, learn and to correct for sequence-specific and fragment-level GC content biases, respectively. Gene expression levels were normalized using the transcripts per million mapped reads (TPM) method, exported as estimated transcript abundance, and aggregated to gene-level expression using the Bioconductor package tximport (version 1.2.0) [55] complemented with the reader package (version 1.1.1), within the R environment (version 3.3.3). Principal component analysis (PCA) was performed in R using ggplot2 (version 2.2.1) and gplots package (version 3.0.1) to determine relationships between samples.

2.4. Differential Expression Analysis

DESeq2 software (version 1.14.1) in R was used to identify DEGs in pairwise comparisons [56]. Two series of DE analysis using the following contrast arguments was performed with the reference assembly approach in flag-leaf and panicle samples: contrast 1—the condition effect for each genotype, in other words, IL_DvsIL_C, and SWA_DvsSWA_C, and contrast 2—the genotypic effect for each condition, in other words, IL_CvsSWA_C and IL_DvsSWA_D. Only genes that have at least ten reads in total were used for DE analysis. Differentially expressed genes (DEGs) were defined as those presenting an absolute fold change (FC) ≥ 2 or ≤ 0.5 and a False Discovery Rate (FDR) adjusted p-value ≤ 0.05 in any pairwise comparison. DEGs were then subjected to enrichment analysis of gene ontology (GO) terms, KEGG, and other metabolic pathways defined by a hypergeometric and Fisher's exact test using agriGO (version 2.0), KOBAS (version 3.0), and STRING database (version 10.5). The MapMan tool (http://MapMan.gabipd.org) was used to visualize the involvement of the DEGs in pathways of interest.

2.5. Gene Co-Expression Network Analysis

Gene co-expression network analysis to group genes into modules used the R package WCGNA (v1.6.1). A power value of 6 and 9 for flag-leaf and panicle, respectively, predicted a gene co-expression network that exhibited scale-free topology with inherent modular features (Figure S10A,D). The "blockwiseModules" function of WGCNA was used to detect and generate modules. Network interconnectedness was measured by calculating the topological overlap using the TOMdist function with a signed TOMType. Average hierarchical clustering using the "hclust" function was performed to group the genes based on the topological overlap dissimilarity measure (1-TOM) of their connection strengths. Network modules were identified using the dynamic tree cut algorithm (version 1.63.1) with minimum and maximum module size of 20 and 20,000, respectively, merging threshold function at 0.15, and deep split parameter set at level 2. The module "eigengenes" was used to calculate the correlation coefficient for the samples to identify biologically significant modules. To visualize the expression profiles of the modules, the eigengene (first PC) for each module

was plotted using a customized bar plot function in R. To identify hub genes within the module, the module membership (MM) for each gene also known as module eigengene-based connectivity (kME) was calculated, based on the Pearson correlation between actual expression values and the module eigengene. Incorporating the gene significance (GS) measures, which could also be defined by the −log10 (*p*-value) from IL_DvsSwa_D contrast in DE analysis as external information into the co-expression network, genes within a module with the highest MM and GS values are highly connected within that module. To identify modules shared between the flag-leaf and panicle networks, a consensus network was generated. An in-house R function was used for overlap counting and statistical testing. The consensus network matrix for the flag-leaf and panicle tissue networks was plotted to show the significant overlap in gene count of two modules based on Fisher's exact test with the −log10 (*p*-value).

2.6. Over-Representation Analysis (ORA)

The "kegga" function under the "goana" package in R utilized the user-supplied GO slim assignment and InterPro classification from RGAP 7 independently in the form of data.frame annotation alongside the multiple gene lists generated in each module. Gene.pathway was the data.frame linking genes to pathways and pathway.names was the data.frame giving full names of pathways. The universe was the vector specifying the set of unique gene identifiers used in WGCNA to be the background and not the whole genome. Finally, GO slim terms, and InterPro protein families and domains were called significantly over-represented in the gene set if the *p*-value is < 0.05.

2.7. Quantitative PCR Analysis

Primers were designed using QuantPrime (https://quantprime.mpimp-golm.mpg.de). cDNA was synthesized from 2 µg total RNA using the ImProm-II Reverse Transcription System (Promega, Madison, WI, USA), according to the manufacturer's protocol. qRT-PCR was performed using two independent biological replicates and three technical replicates. qRT-PCR was set up in 386-well PCR plates with 0.2 µM primers using SYBR Green PCR Master Mix kit (Applied Biosystems, Foster City, CA, USA), following the manufacturer's protocol in a reaction volume of 10 µL via a Roche LightCycler 480 Real-Time system (Rotkreuz, Switzerland). Reaction conditions were as follows: denaturation at 95 °C for 5 min, 45 cycles of 95 °C for 10 s, 60 °C for 15 s and 72 °C for 8 s, heating from 65 to 95 °C. Two internal reference genes ELF and ATU were designed to normalize the relative gene expression levels for flag-leaf and panicle tissue, respectively, using the $2^{-\Delta\Delta}$CT method with ΔCT = CTgene − CTreference gene [57]. For comparison of fold change, scatterplots were generated using the $\log_2$ fold change determined between RNA-Seq and qRT-PCR, which is defined as ΔΔCT (for comparative threshold cycle).

2.8. Genotyping

Using the C7AIR, 7098 SNPs were called for N22, Swarna and the DTY-IL [58]. Frequencies for each SNP across replicated samples were estimated and the most frequent genotype was considered true. Missing markers and monomorphic markers between the parents N22 and Swarna were discarded. For the remaining markers (1648 SNPs) genotypic calls from each parent were used to assign inheritance from N22 or Swarna. Fragments from the donor parent N22 were defined as consecutive SNPs with N22 homozygous genotypes. Markers that potentially represent miss-called double recombination were discarded if the probability of observing this event was smaller than 1 cM or 1 in 100 events. A graphical representation of the markers inherited from N22 and Swarna were graphed using the R package ggplot2. RNA-Seq reads of the candidate genes were aligned and visualized in IGV (version 2.8.2) relative to MSU7 (Nipponbare) and in the latest versions of the MH63 and N22. Clustal Omega (version 1.2.4) was used for multiple protein sequence alignments. FGENESH was used as the gene prediction tool with *O. sativa* vg. *indica* as the background organism. SNP-Seek (https://snp-seek.irri.org) was used to validate the NS SNPs across the 3 K genomes.

2.9. DNA Extraction and Sanger Sequencing

Genomic DNA was extracted from the leaves of N22, the DTY-IL *qDTY* donor, using the Qiagen DNeasy Kit (Qiagen, Limburg, The Netherlands) according to the manufacturer's instructions. LOC_Os01g67030 (auxin responsive protein) including a 1.8 kb upstream promoter region was amplified using the forward primer GAGCGTGCAGTCCACTAGGCATTATC and reverse primer GTGACACGTATTCTGATGTACTG. The amplicon was cloned into the pGEM-T Easy Vector (Promega, WI, USA), as per manufacturer's instructions and Sanger sequenced using Macrogen, Inc. South Korea as service provider.

3. Results

3.1. Phenotypes of Swarna and DTY-IL under Reproductive Stage Drought Stress

In the 2014 and 2015 dry season (DS) drought-stress field trials at IRRI, DTY-IL and Swarna, showed similar grain yield (Figure 1A) and plant height (Figure 1B) under irrigated conditions. Under reproductive-stage drought stress height was reduced in both genotypes to a similar degree (Figure 1B). While yield was reduced in both lines under drought, DTY-IL achieved about double the average grain yield compared to Swarna (Figure 1A). In addition, three weeks after draining the field, Swarna showed clear signs of leaf rolling. Leaf rolling was also observed for Swarna in the greenhouse experiment. While there was no visible difference in flag-leaf morphology between both genotypes under the well-watered condition (Figure 1C), a prominent leaf rolling phenotype in Swarna was observed after ten days of drought stress with complete leaf-rolling on the 12th day of drought stress (Figure 1D).

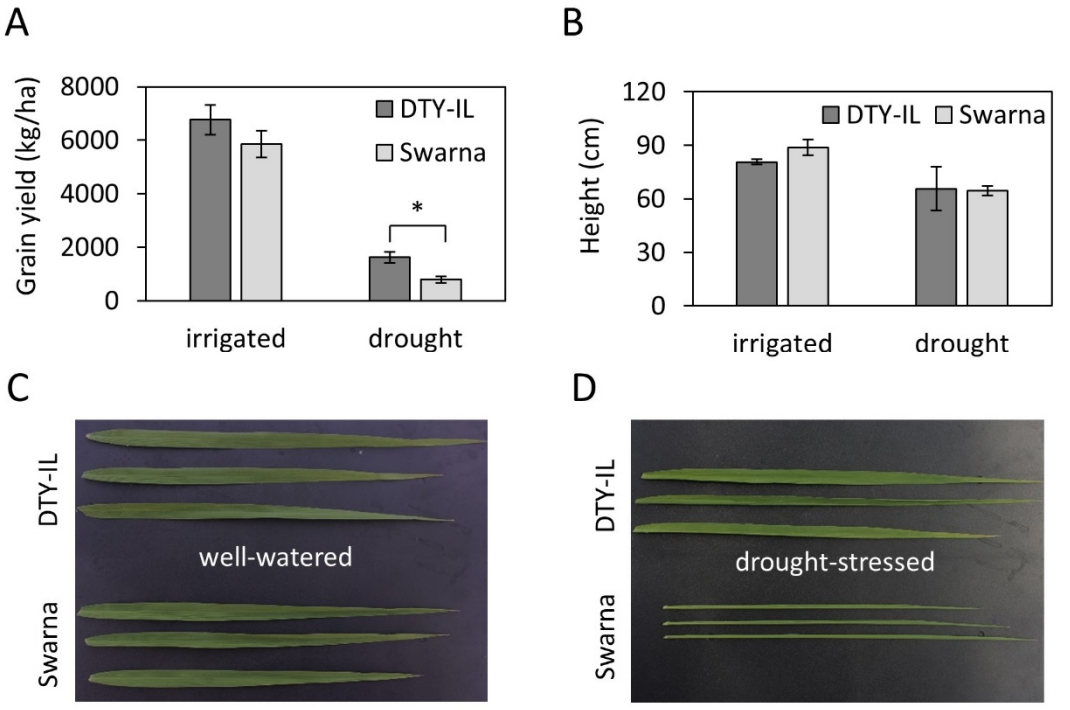

Figure 1. The effect of reproductive stage drought on yield, height and flag-leaf morphology. The average grain yield (**A**) and plant height (**B**) across the 2014 and 2015 dry season (DS) field trial of DTY-Il and Swarna under irrigated and drought condition ($N = 2–9$). Flag-leaf phenotypes of the DTY-IL and Swarna under well-watered conditions (**C**) and the leaf-rolling phenotype during drought-stress (**D**) under controlled greenhouse conditions. The asterisks (*) indicates a significant difference (Student's *t* test, * $p < 0.01$).

3.2. Generating a Transcriptional Map of the Moderate RDS Response in Rice

Mapping rates ranged from 77.7–92.9% for flag-leaf and 87.9–92.8% for panicle (Table S1), covering 28,283 and 33,698 genes, respectively. Sample clustering and heatmap visualization of log_2-transformed, normalized count data demonstrated clear separation between genotypes and treatments for both flag-leaf and panicle samples (Figures S2A,B and S3A,B). Principal components (PC) analysis showed that the first and second PC explained 93% of the total variation for flag-leaf (Figure S2C) and 81% for panicle tissue (Figure S3C). Biological replicates of each genotype-treatment combination clustered together and the treatment effect was greater than the genotype effect for both tissues (Figures S2C and S3C). An exception was a single Swarna panicle sample, which was removed from all further analyses as an outlier (Figure S4). The sum of the non-redundant/unique log_2 normalized genes with significant changes of expression at FDR adjusted p-value ≤ 0.05 across four different contrasts were 17,616 and 18,614 for flag-leaf and panicle tissue, respectively. Pairwise DE analysis for all genotype-treatment combinations identified DEGs of significance for flag-leaf and panicle (Figure S5), and a Venn diagram was used to visualize three categories of unique and common responses in flag-leaf (Figure 2A and Figure S6A,B, Table 1) and panicle (Figure 2B and Figure S6C,D, Table 1).

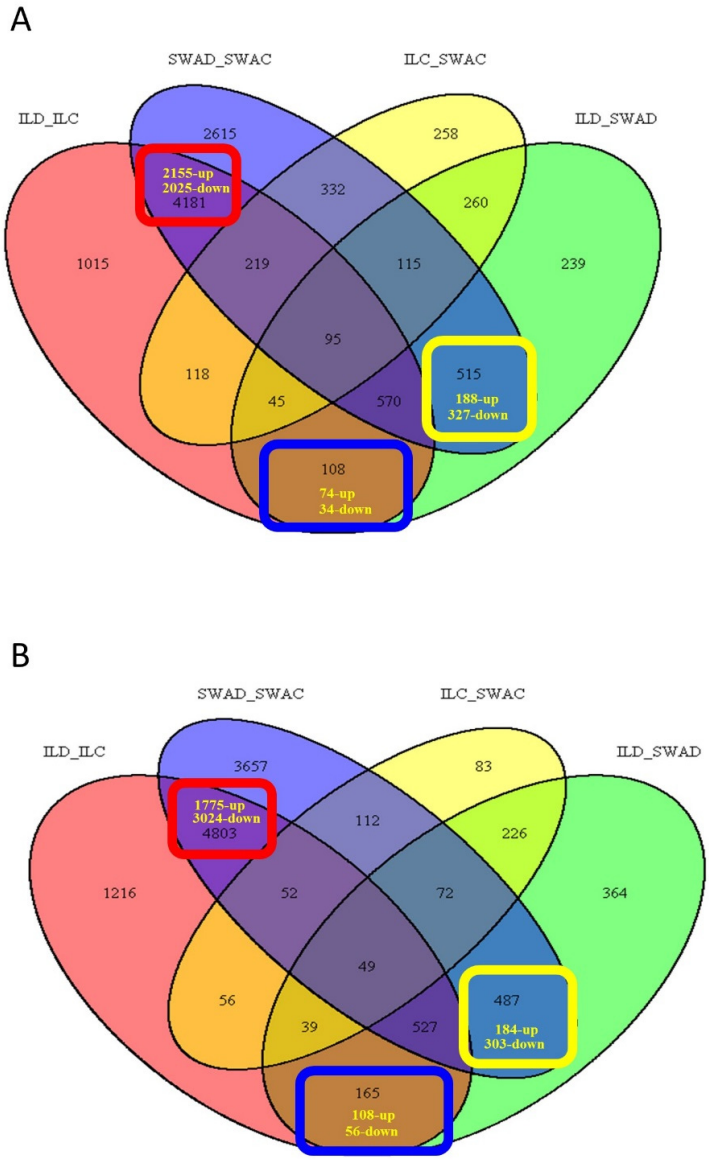

Figure 2. Gene differential expression and identification. Venn diagram of differentially expressed

genes (DEGs) for flag-leaf (**A**) and panicle (**B**) tissues in Swarna and DTY-IL under reproductive drought stress (RDS) at a false discovery rate (FDR) adjusted p-value < 0.05 and $-1 \leq \log_2$-ratio $\leq +1$ (fold change ≥ 2 and ≤ 0.5). The three highlighted boxes for each tissue represent the common DEGs (red), unique to Swarna (yellow), and unique to DTY-IL (blue). SWAC = Swarna control, SWAD = Swarna under RDS, ILC = DTY-IL control, ILD = DTY-IL under RDS.

Table 1. A summary of GO enrichment analysis of differentially expressed genes (DEGs) common to both genotypes, and unique to DTY-IL and Swarna for flag-leaf and panicle tissues under RDS.

DEGs of Interest	Expression	Genes		GO Terms		Significant GO Terms	
		Flag-Leaf	Panicle	Flag-Leaf	Panicle	Flag-Leaf	Panicle
Common responses of DTY-IL and Swarna DEGs to drought	Upregulated	2155	1775	409	324	88	110
	Downregulated	2025	3024	482	525	171	135
	Sub-total	4180	4799	891	849	259	245
Unique responses of Swarna DEGs to drought	Upregulated	188	184	92	89	0	0
	Downregulated	327	303	134	141	35	13
	Sub-total	515	487	226	230	35	13
Unique responses of DTY-IL DEGs to drought	Upregulated	74	108	31	58	4	36
	Downregulated	34	56	19	22	0	0
	Sub-total	108	164	50	80	4	36

3.2.1. Expression Profiles of Drought-Responsive Genes in the Flag-Leaf Tissue under RDS

A total of 4180 genes were found to be drought-responsive in flag-leaves of both Swarna and DTY-IL (Figure 2A, Table 1). Gene ontology (GO) enrichment analysis showed functional enrichment among upregulated DEG for transcription, regulation of biological processes, and oxidation-reduction (Table S2-1), while the shared downregulated DEGs were mainly associated with transmembrane transport, localization, and post-translational protein modification (Table S2-2).

In Swarna flag-leaves a total of 515 (188 up- and 327 downregulated) genes were uniquely drought-responsive (Table 1). While no significant GO terms were detected for upregulated DEGs (Table 1), significant GO terms for uniquely downregulated DEGs were largely related to post-translational protein modification, photosynthesis, defense response, and programmed cell death (Figure S7A). Pathway enrichment suggested photosynthesis, ubiquinone, and other terpenoid-quinone biosynthesis, as well as glutathione-mediated detoxification II and tyrosine biosynthesis (Table S3), to be significantly downregulated. MapMan visualization supported the downregulation of cell wall, carbon metabolism, secondary metabolism, and light reaction in Swarna flag-leaves (Figure 3A and Figure S9A).

In DTY-IL flag-leaves 108 (74 up- and 34 downregulated) DEGs were uniquely drought-responsive. While no significant GO terms could be associated with downregulated DEGs, oxidation-reduction, response to stress, and response to stimulus were among the significant GO terms in upregulated DEGs (Figure S7B). Pathway enrichment suggested phenylpropanoid biosynthesis, dhurrin, xylan, and scopoletin biosynthesis, as well as detoxification of reactive carbonyls in chloroplasts to be uniquely upregulated under RDS (Table S3). This was supported by MapMan visualization, showing upregulation of cell wall, lipids, and secondary metabolism (Figure 3B and Figure S9B).

Numerous overrepresented *cis*-elements were found in the group of 327 promoters of uniquely downregulated DEGs in Swarna in flag-leaf, which are mostly involved as binding sites for dehydration responsive genes. These include ACGTATERD1, IBOX, PREATPRODH, MYCATERD1, MYCATRD22, CCAATBOX1, and MYB2AT (Table S4-1). The overrepresented motifs in a set of 74 promoters in the uniquely upregulated DEGs in IL in flag-leaf were mostly functioning upon induction of dehydration stress through the ACGTATERD1 motif (Table S4-2).

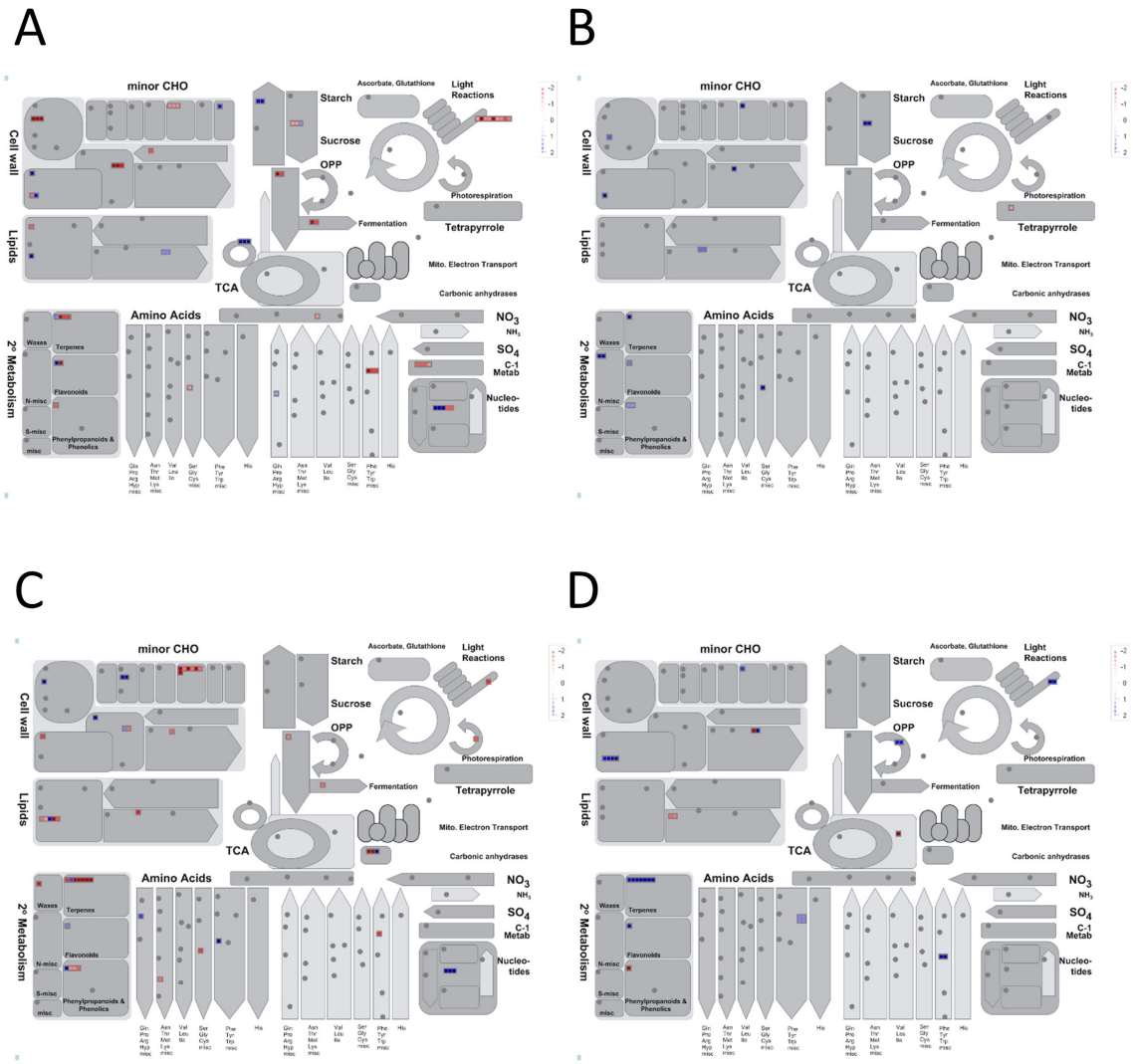

Figure 3. Mapman overview of the DEGs of interest in DTY-IL and Swarna under RDS. The metabolism overview in in the flag-leaf tissue for Swarna (**A**) and DTY-IL (**B**), as well as for the panicle tissue in Swarna (**C**) and DTY-IL (**D**). The DEGs were binned to the MapMan functional categories. The values are the $\log_2$ fold changes. Upregulated categories are represented in blue and downregulated categories in red.

3.2.2. Expression Profiles of Drought-Responsive Genes in the Panicle Tissue under RDS

A total of 4799 genes were found to be drought-responsive in panicles of both Swarna and DTY-IL (Figure 2B; Table 1). Enriched GO categories of the upregulated DEGs related to post-translational protein modification and response to stress (Table S5-1), while enriched GO terms of the downregulated DEGs were mostly related to transmembrane transport, carbohydrate metabolic process, and localization (Table S5-2).

In Swarna panicles, a total of 487 (184 up and 303 downregulated) genes were found uniquely drought-responsive (Table 1). No significant GO terms were identified within the uniquely upregulated DEGs. For the uniquely downregulated genes, significant GO terms included oxidation-reduction as well as monooxygenase activity, tetrapyrrole, and heme-binding (Figure S8A). Significantly enriched pathways associated with downregulated DEGs were related to DNA replication, diterpenoid biosynthesis, phenylpropanoid biosynthesis, and photosynthesis (Table S6). MapMan visualization supported the downregulation of cell wall, lipids, secondary metabolism, amino acids, as well as carbohydrate metabolism (Figure 3C and Figure S9C).

In DTY-IL panicle 164 (108 up and 56 downregulated) DEGs were uniquely drought-responsive (Table 1). No significant GO enrichment was identified among the uniquely downregulated DEGs of DTY-IL. Prevalent GO terms of upregulated DEGs were related to protein amino acid phosphorylation as well as oxidation-reduction and carbohydrate metabolic processes (Figure S8B). The most significantly enriched pathways in the panicle tissue of DTY-IL upregulated DEGs were related to propanoate metabolism, methylerythritol phosphate pathway, diterpenoid biosynthesis, camalexin biosynthesis, and circadian rhythm in plants (Table S6). This was supported by MapMan visualization, showing upregulation of cell wall, lipids, secondary metabolism as well as amino acids (Figure 3D and Figure S9D).

Overrepresented *cis*-acting elements in the group of 303 promoters of the uniquely downregulated DEGs in Swarna in panicle tissue mostly involved in dehydration response like the ACGTATERD1, MYBCOREATCYB1, ABRELATEDRD1, and IBOX motifs (Table S7-1). Overrepresented *cis*-elements in a set of 108 promoters of uniquely upregulated DEGs in DTY-IL in panicle tissue were mostly related to dehydration response like the MYB2AT, MYBCOREATCYCB1, and ACGTABOX (Table S7-2).

3.3. Drought-Stress-Related Gene Modules within the Transcriptional Map

WGCNA identified 21 distinct co-expressed modules with different expression patterns in flag-leaf (designated as FL-M1 to FL-M21, capturing 17,616 genes) (Figure S10B,C), and 23 distinct modules for panicle network (designated as P-M1 to P-M23, capturing 18,614 genes) (Figure S10E,F).

More than 70% of genes were distributed in the FL-M1 and FL-M2, and P-M1 and P-M2 (common response between DTY-IL and Swarna under RDS and control) for flag-leaf and panicle networks, respectively (Table S8-1,S8-2; Figure S11), signifying a common response shared between Swarna and DTY-IL. Modules FL-M1 and FL-M2 in the flag-leaf network showed "localization" and "transport" as the most enriched GO terms (Table S9-1). In the panicle network, P-M1 genes were enriched for functions related to "RNA processing" while the P-M2 module was linked with "localization" and "transport" (Table S9-2).

3.3.1. Flag-Leaf Specific Modules

Two specific flag-leaf modules with a contrasting pattern of expression were investigated in more detail for implications in the differential performance of the two genotypes under RDS. FL-M14 consisting of 140 genes (Table S10-1) had significantly higher expression profiles in all samples of the DTY-IL genotype under RDS, whereas a lower expression across the three other groups of samples was observed (Figure 4A). FL-M16 consisting of 102 genes (Table S10-2) had significantly lower expression in Swarna under RDS, whereas the three other groups of samples had a higher expression (Figure 4B).

FL-M14 enriched BP GO terms were "cellular amino acid biosynthetic process" as well as "cell wall organization or biogenesis" (Figure S12A). The enriched pathway included "biosynthesis of secondary metabolites", "fatty acid elongation", and "phagosome" while the overrepresented Interpro domains included "Expansin" as well as "Glycosyl transferase, family 43", and "Plant peroxidase" (Figure 5A). FL-M14 hub genes included amidase and expansin (Figure S13A; Table S11-1). Interestingly, numerous cell wall organization and biogenesis genes are upregulated in DTY-IL and downregulated in Swarna under RDS (Figure 6).

FL-M16 was enriched in "oxidation-reduction process" as well as "cellular carbohydrate metabolic process" (Figure S12B). The enriched pathways include "photosynthesis", "folate biosynthesis", and "vitamin B6 metabolism" while the overrepresented Interpro domains in FL-M16 included "Ferrodoxin—NAP reductase", "Multicopper oxidase", and "Photosystem antenna protein-like" (Figure 5B). FL-M16 hub genes included OsSub37—putative subtilisin homologue and cytochrome P450 (Figure S13B; Table S11-2).

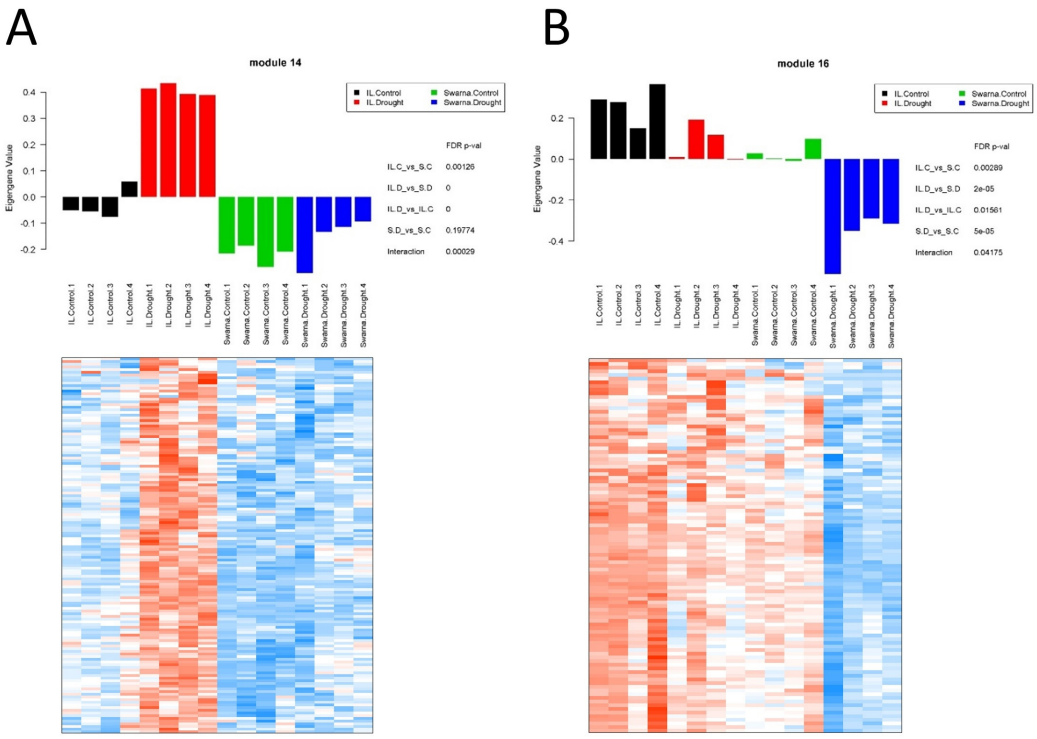

Figure 4. Gene co-expression network analysis in flag-leaf under RDS. Bar plots of the module eigengene as representatives of gene expression profiles across samples in FL-M14 (module 14) (**A**) and FL-M16 (module 16) (**B**). *X*-axis represents 16 different samples across four different groups, while *Y*-axis corresponds to the eigengene value. Heatmaps showing gene expression levels of genes in FL-M14 and FL-M16. Columns represent samples, while rows correspond to genes in the module. Red indicates positive and blue negative expression profile. S.C = Swarna control, S.D = Swarna under RDS, IL.C = DTY-IL control, IL.D = DTY-IL under RDS.

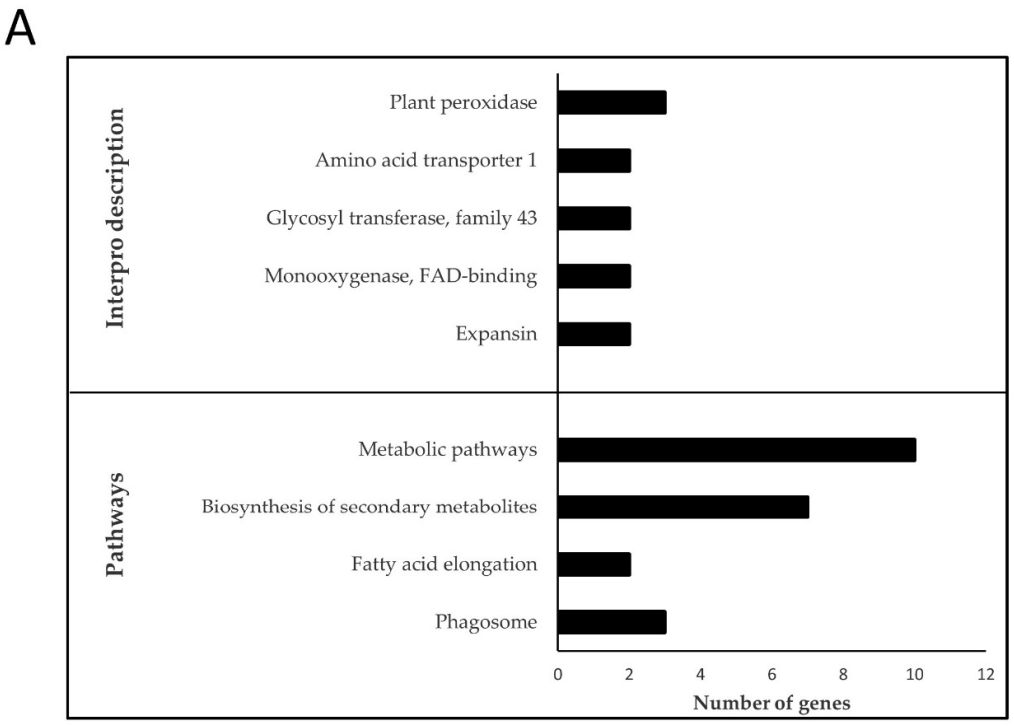

Figure 5. *Cont.*

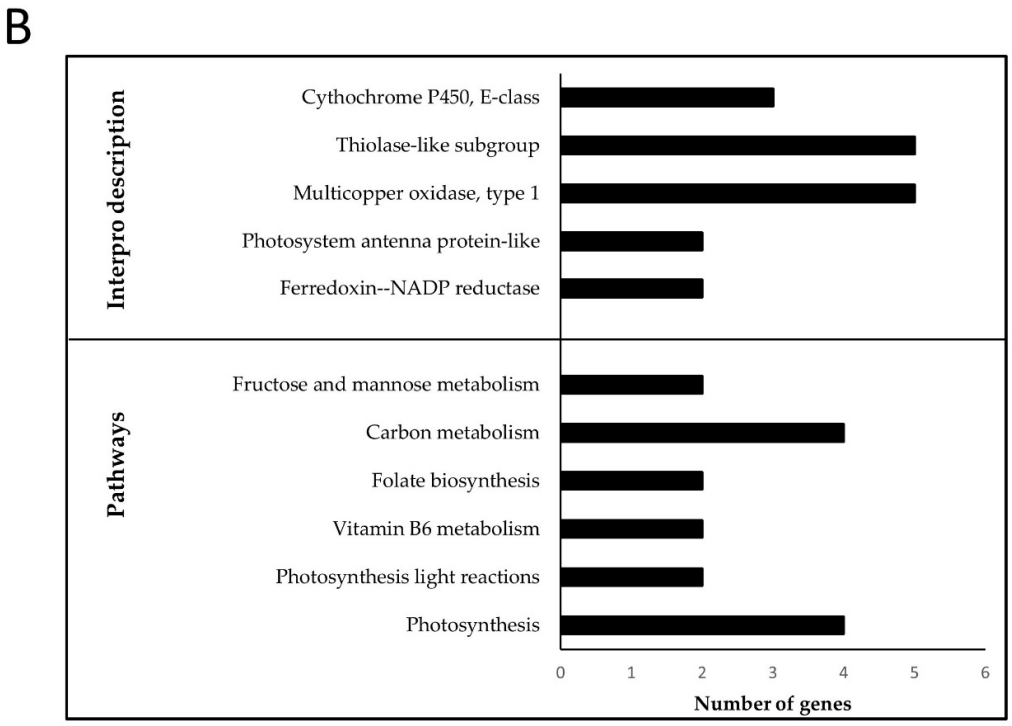

Figure 5. Enrichment analysis of the functional categories in FL-M14 and FL-M16. Over-represented Interpro domains and enriched pathways in FL-M14 (**A**) and FL-M16 (**B**) in flag-leaf under RDS. Top significant pathways and Interpro domains are shown in *Y*-axis with the number of represented genes on the *X*-axis.

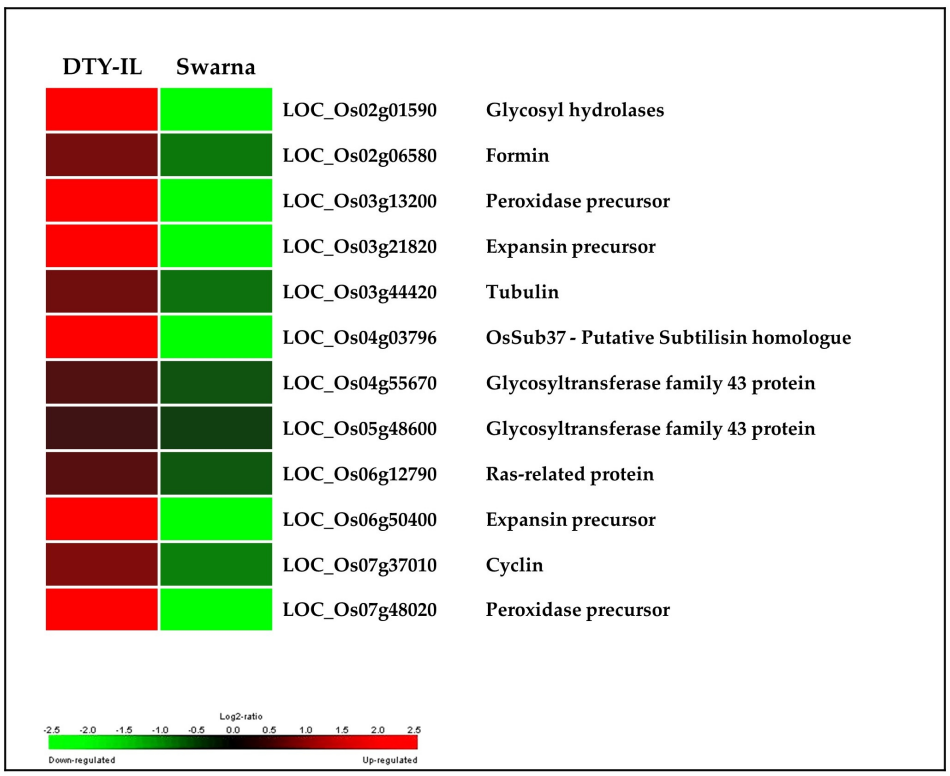

Figure 6. Cell wall organization and biogenesis during RDS in the flag-leaf tissue. Expression of cell wall organization or biogenesis related genes in drought-responsive modules between DTY-IL and Swarna are shown as $\log_2$ fold change heat-maps.

3.3.2. Panicle Specific Modules

Two contrasting panicle modules (P-M10 and P-M15) were investigated in more detail. P-M10 consisting of 138 genes (Table S12-1) and P-M15 consisting of 73 genes (Table S12-2) had significant interaction with drought response in a genotype-specific manner. P-M10 had significantly higher expression profiles in all samples of DTY-IL under RDS and a lower expression pattern across the other three groups of samples (Figure 7A). P-M15 had significantly lower expression profiles in all samples in Swarna under RDS, whereas the three other groups of samples had a higher expression (Figure 7B).

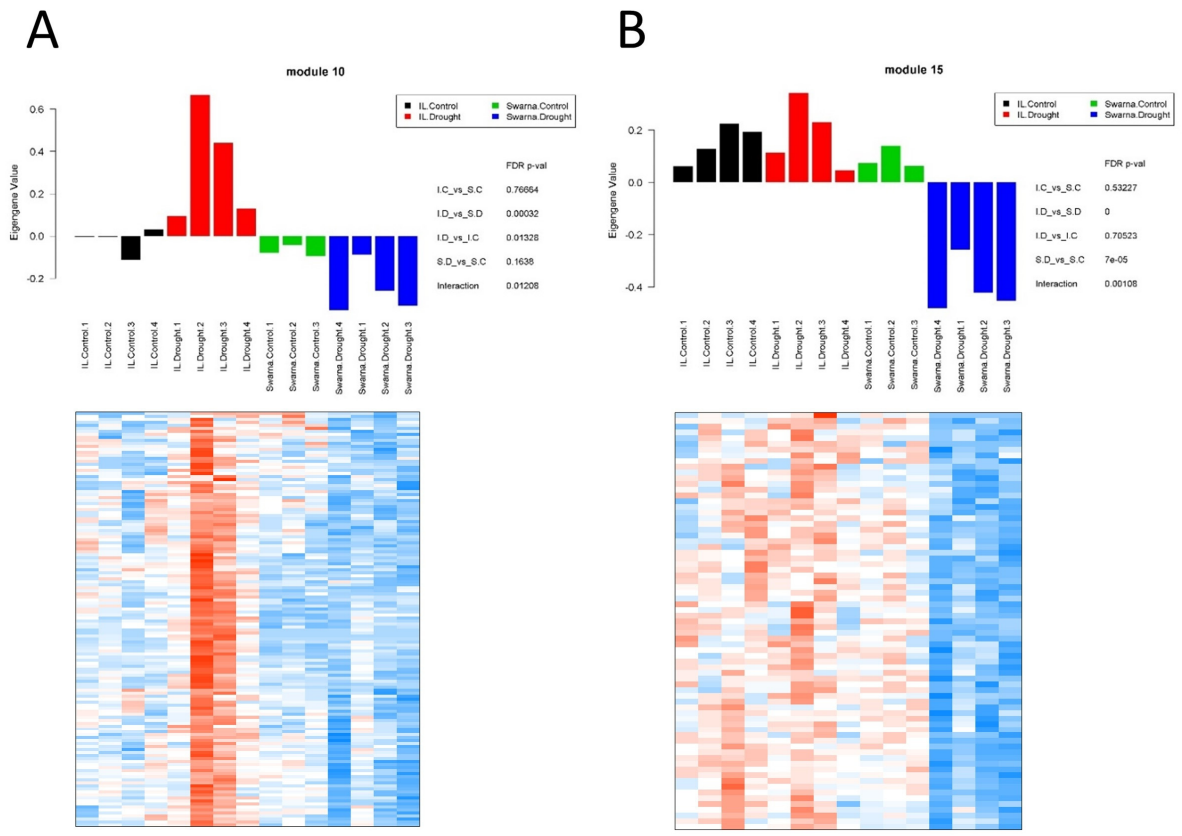

Figure 7. Gene co-expression network analysis in panicle under RDS. Bar plot of the module eigengene as representatives of the gene expression profiles across different samples in P-M10 (module 10) (**A**) and P-M15 (module 15) (**B**). *X*-axis represents 15 different samples across four different groups, while *Y*-axis corresponds to the eigengene value. Heatmaps showing gene expression levels of genes in P-M10 and P-M15. Columns represent samples, while rows correspond to genes in the module. Red indicates positive and blue negative expression profile. S.C = Swarna control, S.D = Swarna under RDS, IL.C = DTY-IL control, IL.D = DTY-IL under RDS.

P-M10 enriched BP GO terms were "calcium ion transmembrane" as well as "lipid biosynthetic process" (Figure S14A). Pathway enrichment analysis included "glutathione metabolism", "phenylpropanoid biosynthesis", and "ribosome" while the overrepresented Interpro domains were "Protein kinase" as well as "Plant peroxidase" (Figure 8A). P-M10 hub genes included OsWAK receptor-like cytoplasmic kinase and a serine-type peptidase (Figure S15A; Table S13-1). Analysis of genome-scale metabolic pathways in the DTY-IL revealed the up-regulation of genes involved in the biosynthesis of antioxidant enzymes and metabolites (Figure 9 and Figure S14).

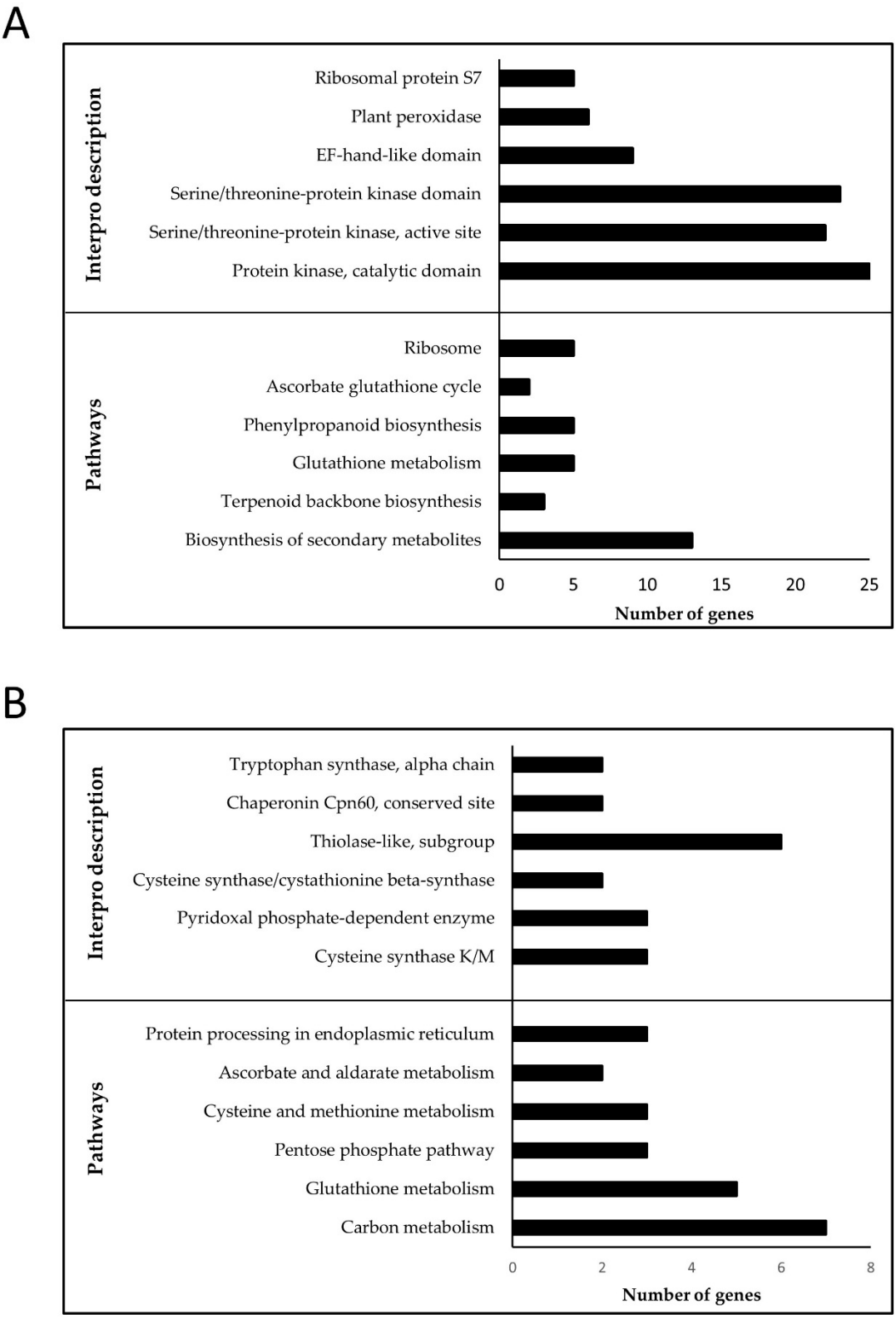

Figure 8. Enrichment analysis of the functional categories in P-M10 and P-M15. Over-represented Interpro domains and enriched pathways in P-M10 (**A**) and P-M15 (**B**) in panicle under RDS. Top significant pathways and Interpro domains are shown in *Y*-axis with the number of represented genes on the *X*-axis.

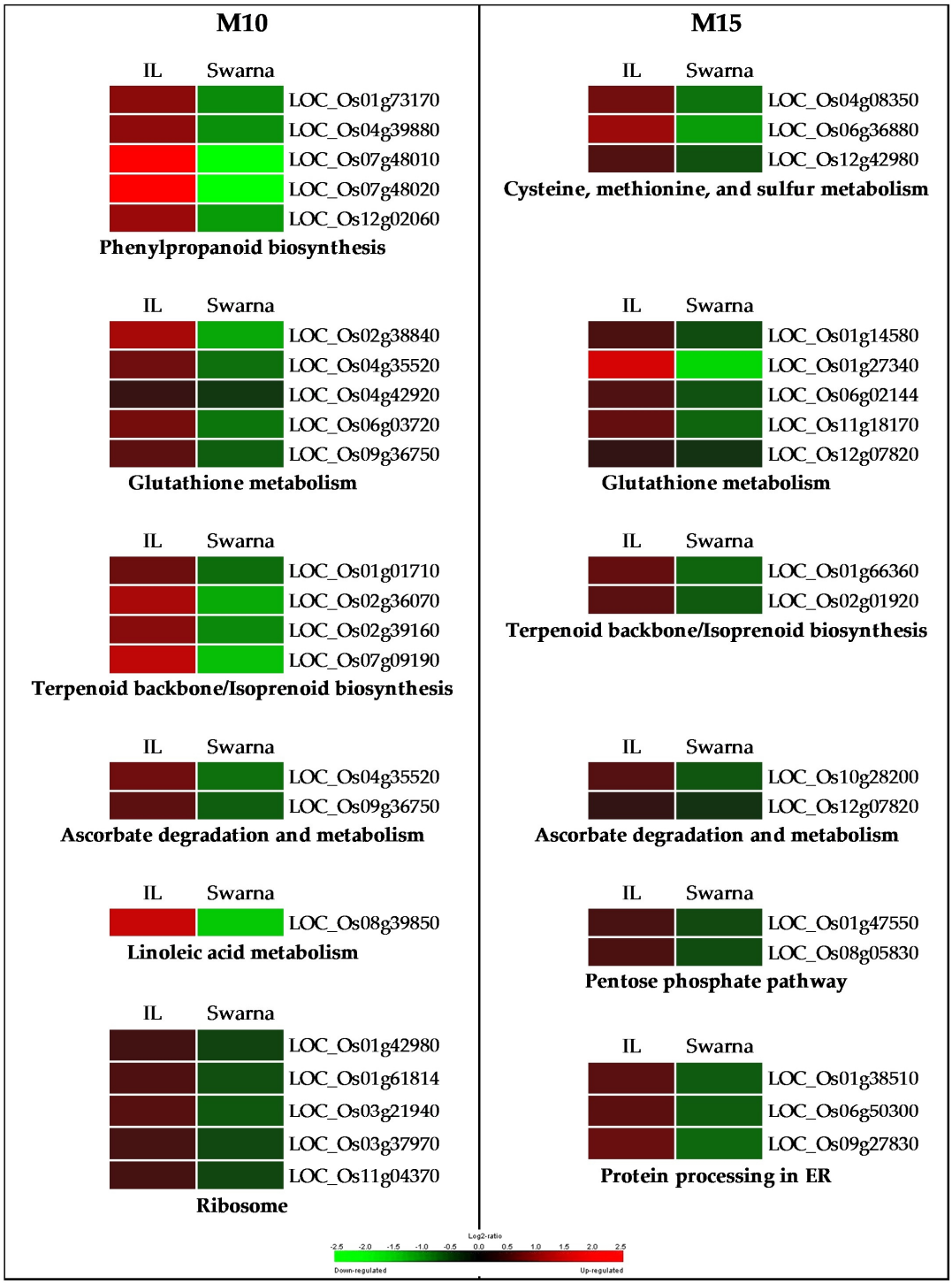

Figure 9. Regulation of metabolic pathways during RDS in panicle. The metabolic pathways enriched in the drought-responsive modules P-M10 (M10) and P-M15 (M15) between DTY-IL and Swarna under RDS are shown in heat-maps representing their expression profile. The scale represents a $\log_2$ fold change in expression. IL = DTY-IL.

P-M15 were GO enriched for "carboxylic acid metabolic process" as well as "coenzyme metabolic process" (Figure S14B). The enriched pathways includes "carbon metabolism", "glutathione metabolism", and "pentose phospate pathway" while the overrepresented Interpro domains included "Cysteine synthase" and "Thiolase-like, subgroup" (Figure 8B). P-M15 hub genes included the glycosyl hydrolase family 29, and dehydrogenase/reductase (Figure S15B; Table S13-2).

The consensus network from the flag-leaf and panicle transcriptomes contained few significant overlaps in module classifications between the flag-leaf and panicle networks, consistent with the tissue-specific expression under RDS [23] (Figure S16). Similarly, colored modules between the flag-leaf and panicle networks contained a few significant overlaps of genes with a common consensus network module, consistent with their similar eigengenes profiles (Figures S10 and S11). The significant overlap portrays a common expression pattern for each condition of both genotypes (FL-M1 and P-M1, and FL-M2 and P-M2) and a common expression pattern for each genotype on both conditions (FL-M6 and FL-M7, and P-M5 and P-M6) in the flag-leaf and panicle networks, respectively.

3.4. Validation of Differential Gene Expression

RNA-Seq results were validated using ten genes from different response categories (increased, decreased, and non-differentially expressed genes upon treatment in both flag-leaf and panicle) for qRT-PCR (Figure S17A,B). Three selected genes from within the *qDTY1.1* region (LOC_Os01g66120, LOC_Os01g66820, and LOC_Os01g67030) showed differential expression. LOC_Os01g66120 (no apical meristem protein) was upregulated in both genotypes and both tissues under drought. LOC_Os01g66820 (inactive receptor kinase At1g27190 precursor) was downregulated in DTY-IL flag-leaves under RDS. LOC_Os01g67030 (auxin responsive protein) was upregulated under RDS in DTY-IL panicles and downregulated in Swarna panicles but not affected by RDS in flag-leaves. A high correlation between qRT-PCR results and RNA-Seq results was observed for flag-leaf (R^2 = 0.88) and panicle (R^2 = 0.91) tissues (Figure S17C,D), supporting RNA-Seq-based findings and interpretations. Targeted transcripts and respective primer sets used are shown in Table S14.

3.5. Colocalization of DEGs in the Introgression Fragments

SNP genotyping revealed 16 N22-derived fragments in DTY-IL (Figure 10). The largest fragment was found on chromosome 1, encompassing *qDTY*1.1, followed by an introgression on chromosome 3, containing parts of *qDTY*3.2, which was also reported as N22-derived in an N22 by Swarna population [7]. Additional introgressions on chromosomes 4, 8, 9, and 10 did not overlap with major DTY QTL. Overlaying DEGs on the N22 introgressions identified 463 DEGs in the flag-leaf (Table S15-1) and 433 DEGs in the panicle (Table S15-2), of which 6 overlapped with the fine mapped region of *qDTY*1.1 [59], while 5 overlapped with the *qDTY*3.2 region.

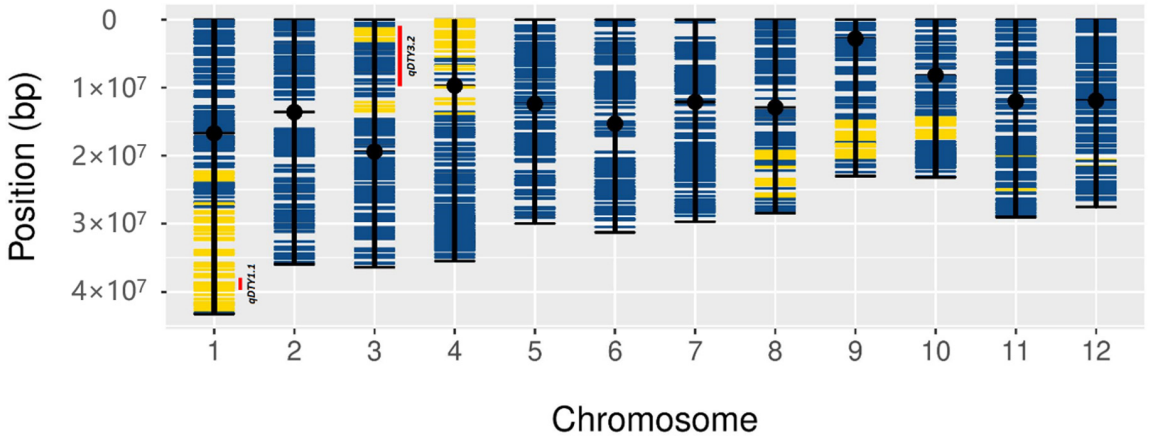

Figure 10. Physical map of DTY-IL. Genome-wide physical position distribution of 1648 SNPs from the 7K genotyping assay across all rice chromosomes. Swarna SNP's alleles are represented in blue. N22 SNP alleles are represented in yellow. Names and ranges of N22-derived DTY QTLs (*qDTY*1.1 and *qDTY*3.2) are shown as red bars on the sides of the chromosome, more details are provided in Supplementary Table S15.

Of the 6 DEGs in the *qDTY*1.1 region (Table S16-2), LOC_Os01g67030 was upregulated in the panicle (Log_2 fold change = 3.1), was annotated as an auxin-responsive protein of 418 amino acids (AA) in Nipponbare. While LOC_Os01g67030 was annotated in the *indica* reference MH63v2, it was missing in the N22v2 reference genome. FGENESH-based gene prediction in N22v2 revealed a putative homologue showing 91.4% identity with Nipponbare and 92.3% identity with MH63v2. Differences were found in the 5′UTR, resulting in the loss of coding sequence for the first 37 AA in the MH63v2 and N22v2 alleles, as well as a number of nonsynonymous (NS) SNPs (Figure S18). NS SNPs unique to N22 corresponded to four AA changes (P52L, C60F, S80T, Q137P) and an AA deletion (G253del) (Figure S19). While the alignment of the 2 kb upstream *cis*-regulatory region of LOC_Os01g67030 in Nipponbare and MH63v2 showed a 99.1% identity, N22v2 displayed a large deletion, including the 5′UTR. With an identity of less than 15% to either Nipponbare or MH63v2, the N22v2 *cis*-regulatory region of LOC_Os01g67030 was distinct with unique regulatory elements (Table S17) that could explain the observed expression differences.

Of the 5 DEG within *qDTY*3.2, LOC_Os03g03510, downregulated in the panicle (Log_2 fold change = −1.11617), was annotated as CAMK_KIN1/SNF1/Nim1_like.15-calcium/calmodulin-dependent protein kinase in Nipponbare, with corresponding annotations in MH63v2 and predictions in N22v2. LOC_Os03g03510 contains a sucrose non-fermenting 1-related kinase 3 (SnRK3) domain and a CBL-interacting serine/threonine-protein kinase 3 (CIPK3) domain. While the coding sequences were largely conserved in multiple sequence alignment between Nipponbare, MH63v2, and N22v2 alleles, the N22v2 allele featured an altered stop codon resulting in a 35 AA C-terminal extension (Figure S20).

4. Discussion

Source-sink relationships largely determine the grain yield of cereal crops, with developing grains being primary sinks, while the top two leaves, the flag-leaf, in particular, serves as the primary source [60,61]. Source sink regulation is orchestrated through intricate metabolic signaling [62], of which key players in sucrose sensing (e.g., trehalose-6-phosphate) and signal integration (e.g., SnRK1) are beginning to emerge [62]. Drought stress affects these relationships by reducing both source and sink strengths. In source organs, limitations in carbon fixation and primary metabolism lead to reduced resource allocation to developing sinks, causing yield reduction characterized by suboptimal grain filling [63]. In sink organs, drought reduces fertility, causing yield reductions through suboptimal seed setting [64].

While DTY-QTLs have demonstrated effects to improve rice grain yields under RDS, knowledge about underlying molecular mechanisms is limited. Functional studies of *qDTY12.1* suggested an intricate pattern of below-ground contributions [18], while physiological studies of *qDTY1.1* suggested above-ground implications [59]. Though confined to a single time point at the late booting stage (close to anthesis) after two weeks of RDS, our study suggested that DTY controlled mechanisms improve yield under drought by acting at both source and sink organs. At the flag-leaf, a coordinated response to sustain primary metabolism through cell wall loosening and maintained photosynthetic rates seems to allow for sufficient carbon and energy allocation to the developing panicle, which in turn enable reproductive structures to invest in protective mechanisms, including protein stabilization and turnover, ROS scavenging and production of protective secondary metabolites. While proximate effects in the panicle are suggested as improved male fertility and improved sink strength under RDS, the ultimate effects are improved seed setting and grain filling, and consequently, drought-tolerant yield (DTY) (Figure S21).

4.1. Source Effects—Flag-Leaf-Specific Differences between DTY-IL and Swarna

Collectively WGCNA and DE analyses suggested a complex interplay of a range of processes in the flag-leaf to contribute to the observed differences in RDS tolerance between DTY-IL and

Swarna. These included specific protein turn-over, cell wall loosening, efficient ROS scavenging, and maintenance of photosynthesis (Figures 4–6 and Figure S12).

A direct consequence of drought is impaired cell turgor [65], which is countered by the stiffening of cell walls to provide structural resistance [66,67]. Prolonged drought stress challenges plants to modify their cell walls, resulting in both cell wall tightening and loosening. Tightening occurs in tissues that are of relevance to structural integrity, while loosening occurs in tissues that need to be maintained in a growing and metabolically active mode [66].

Leaf rolling, a common indicator of drought stress in rice [68] was prominent in Swarna under drought but nearly absent in DTY-IL (Figure 1D). Leaf rolling likely relates to aberrant cell turgor and cell wall homeostasis and phenotypically reflects findings in the flag-leaf specific module M14.

Cell wall organization or biogenesis genes showed an increase in expression in FL-M14. A total of 12 cell wall-related genes were significantly upregulated in the DTY-IL and significantly downregulated in Swarna (Figure 6). These included two glycosyltransferase family 43 proteins, previously reported being involved in the synthesis of glucuronoxylan hemicellulose of secondary cell walls [69] and two expansin genes. Expansins facilitate loosening and extension of plant cell walls by disrupting non-covalent bonding between cellulose microfibrils and matrix glucans [70] and implications in response to dehydration are well documented [71–75] and rose [76].

Higher expression of cytoskeleton and cell cycle-related genes in DTY-IL (Figure 6) further supported the concept of maintained cell growth and stability in the tolerant flag-leaf tissue. Contrastingly, cytoskeletal genes (tubulin and formin) and a cell cycle gene (cyclin) were significantly downregulated in Swarna (Table S10-1).

Several classes of enzymes control ROS production in the cell wall, most prominently plasma membrane NADPH oxidases [77] and class III peroxidases (CIII Prxs) [78]. CIII Prxs are secreted in the extracellular space, where they perform either cell wall stiffening through the peroxidative cycle [79] or cell wall loosening through the hydroxylic cycle [80,81]. In the present study, three CIII Prxs (LOC_Os03g13200, LOC_Os07g01370, and LOC_Os07g48020) were present in FL-M14 (Table S10-1), with LOC_Os03g13200 and LOC_Os07g48020 significantly upregulated in DTY-IL and significantly downregulated in Swarna (Figure 6). High CIII Prxs expression in DTY-IL could support the generation of $^{\bullet}OH$ for cell-wall loosening through cleavage of cell wall polymers [67]. Interestingly, decreased expression of a calcium-dependent NADPH oxidase in Swarna and increased in activity of the DTY-IL in FL-M16 (Table S10-2) was also observed. It is also known as respiratory burst oxidase, and is a well-studied enzymatic source of superoxide [82,83], which had previously been implicated in drought and high-temperature stability [83]. Hence, loosening of the cell wall and synthesis of structural constituents together is suggested to contribute to tolerance of water-deficit in the flag-leaf of DTY-IL.

More effective ROS scavenging, in general, seemed to be an important mechanism differentiating drought responses of Swarna and DTY-IL. Higher expression of peroxiredoxin in DTY-IL (Table S10-2) suggests increased reduction capacity for H_2O_2, indicating enhanced detoxification in drought-stressed leaves.

A primary detrimental effect of water stress in source tissues is impaired photosynthesis [84]. Reduced abundance of photosynthesis-related proteins in response to RDS had previously been reported [85] and was indeed reflected in drought-stressed leaves of RDS-susceptible Swarna (FL-M16). Components of the light reaction (two photosystem genes, components of the core complex of photosystem II (PSII) involved the primary light-induced photochemical processes), the dark reaction (ribulose bisphosphatase and the fructose-1,6 bisphosphatase), and photorespiration (ribulose bisphosphate carboxylase large chain precursor) were found to be consistently downregulated in Swarna (Table S10-2), suggesting functional impairments of general photosynthesis. Protection of photosynthesis from photoinhibition through photorespiration is a well-characterized drought response and furthermore prevents ROS accumulation in green tissues [86]. In addition, Swarna showed a lower expression of two ferredoxin-NADP genes, involved in thylakoid electron transport, suggesting reduced capacity in regulating the relative amounts of cyclic and non-cyclic electron for

ATP and redox homeostasis [69]. Consequently, it is argued that the physiological environment in DTY-IL under RDS supports relatively higher rates of photosynthesis, which in turn, might sustain higher rates of energy and carbon production to support primary metabolism and source strength, ultimately leading to improved grain filling.

4.2. Sink Effects—Panicle Specific Differences between DTY-IL and Swarna

Collectively WGCNA and DE suggested a number of distinct mechanisms to contribute to differences in RDS tolerance between DTY-IL and Swarna in panicles. They included protein stabilization and turnover, ROS scavenging, biosynthesis of secondary metabolites for protection of reproductive organs, and hormonal signaling presumably to adapt reproductive developmental processes to drought. Under field conditions, they resulted in an approximate doubling of yield under drought for DTY-IL as compared to Swarna (Figure 1A), at no significant difference in plant height (Figure 1B).

Dehydration stress enhances the production of ROS and ROS-associated peroxidation causing damage to cellular structures [87]. Being essential for cellular signaling, ROS homeostasis depends on the balance between ROS production and scavenging [82]. Analysis of genome-scale metabolic pathways in the DTY-IL revealed the up-regulation of genes involved in the biosynthesis of antioxidant enzymes and metabolites (Figures 8 and 9 and Figure S14).

Secondary metabolite production is crucial in stress-adaptive mechanisms [88]. Genes in pathways involved in secondary metabolite biosynthesis, lipid biosynthesis, redox homeostasis, amino acid metabolism, carbohydrate metabolism, and protein metabolism were upregulated at the maximum booting stage under RDS in DTY-IL and downregulated in Swarna for P-M10 and P-M15 (Figure 9). Several metabolic pathways found to be shared between the two modules include glutathione, terpenoid, and ascorbate metabolism.

De novo protein synthesis and turnover is fundamental for plants to cope with drought stress [85]. Translational efficiency is affected by ribosome composition, thus relative ribosomal protein abundance can modulate plant environmental responses [89]. Similarly, drought-responsive peptidases and heat shock proteins can alter the active proteome to cope with stress [85,90]. In P-M10 five ribosomal protein-related genes, six protein degradation-related genes (among them four peptidases), and two genes related to protein folding and repair displayed higher expression in DTY-IL (Figure 9; Table S12-1). Congruently reduced expression of two peptidases and three genes related to protein processing, including a heat shock protein was observed for Swarna in P-M15 (Figure 9; Table S12-2). Collectively this suggested that panicles of DTY-IL were more responsive and had the necessary energy to adapt its proteome to drought conditions than Swarna.

In P-M10, six genes involved in the ROS scavenging (two ascorbate peroxidases and four peroxidase precursors) had elevated expression profiles in the DTY-IL (Figure 9; Table S12-1). Efficient reduction of H_2O_2 by peroxidases had previously been implicated with drought-tolerance in rice [19]. Specifically, plant ascorbate peroxidases (APXs) are crucial for ROS homeostasis [91] and free radical detoxification though the ascorbate-glutathione cycle [92], and their functional role in rice drought tolerance was demonstrated through transgenic approaches [91]. In P-M15 three ROS scavenging genes (1 glutathione *S*-transferase, 1 glutathione peroxidase, and 1 stromal ascorbate peroxidase) had a lower expression profile in Swarna (Figure 9; Table S12-2). Glutathione peroxidase (GPX) catalyzes the reduction of H_2O_2 using thioredoxin (Trx), while glutathione *S*-transferases (GSTs) are key to the removal of xenobiotic compounds [85]. Ectopic expression of a GST in *Arabidopsis* [93] and a GPX in rice [94] resulted in enhanced drought tolerance, suggesting functional implications.

Interestingly, an ABC function gene with AP2 domain-containing protein (LOC_Os07g22770) controlling floral organ identity was downregulated in Swarna RDS under P-M15 (Table S12-2), suggesting a link to aberrant Swarna floral development under drought [95]. TFs belonging to AP2 and MYB family are involved in panicle development as well as water-deficit stress response, implying that they may represent a crosstalk component between redevelopment and stress.

A negative regulator of plant drought tolerance in abscisic acid (ABA) signaling, protein phosphatase 2C (PP2C) [96], was upregulated in the DTY-IL in P-M10 (Table S12-1). PP2C inhibits the activity of sucrose non fermenting 1 related kinase 1 (SnRK1) [97], a central integrator of metabolic signaling and regulator of starvation response. Thus, the higher expression of PP2C in DTY-IL might correlate with reduced SnRK1 activity, indicative of anabolism rather than catabolism and thus growth rather than the starvation mode in panicles of DTY-IL.

Brassinosteroids (BRs) are growth-promoting steroid hormones important for male fertility and pollen development [98]. BR catabolism is controlled by BAS1, a cytochrome P450 monooxygenase [99]. BRs bind to the extracellular domain of a cell-surface receptor kinase, BRASSINOSTEROID INSENSITIVE1 (BRI1) to activate kinase activity [100,101]. In P-M10, a BAS1-orthologue and two BRI1 genes were found to be upregulated in DTY-IL (Supplementary Table S12-1), suggesting a role for BR signaling in the maintenance of male fertility as part of the *qDTY*1.1-mediated RDS responses.

4.3. qDTY1.1-Specific Contributions to Drought Tolerance

Of the 16 N22-derived introgressions in DTY-IL, two overlapped with known *qDTY*s for which N22 was a known donor [21]. While the large introgressions on chromosome 1 contain the full *qDTY*1.1 region, a smaller introgression on chromosome 3 partially overlaps with *qDTY*3.2 (Figure 10). Working under the assumption that the genome-wide changes in transcriptomes between the drought-tolerant and drought susceptible genotypes in both flag-leaves and panicle, would at least partially trackback to either transcriptional or allelic differences of specific loci within the *qDTY* regions we took a closer look at the *qDTY*1.1 fine mapped region and *qDTY*3.2 overlap.

Based on the Nipponbare reference, the fine-mapped *qDTY*1.1 region encompasses 79 genes, of which six were differentially expressed between DTY-IL and Swarna under RDS in either tissue (Table S15). An auxin-responsive protein (LOC_Os01g67030), specifically upregulated in DTY-IL panicle under RDS was considered as a likely causative candidate. Generally, auxin has been shown to negatively regulate drought adaptation in plants [63]. Notably, the DEEPER ROOTING 1 (DRO1) promoter was shown to contain auxin-responsive elements (AuxRes) and negatively regulated by auxin [102]. While two AuxRes were found in the LOC_Os01g67030 promoter of Nipponbare and MH63v2 (-513 bp and -1606 bp) only one was found at position -1573 bp in N22v2. The absence of the proximal AuxRe motif, in addition to the presence of novel, putative drought-responsive elements (Figure S18) could explain the observed differential regulation of LOC_Os01g67030 under RDS in DTY-IL.

LOC_Os01g67030.1 contains a cytochrome b561 (Cyt_b561) and a dopamine β-monooxygenase (DOMON) domain (Figure S19). Cyt_b561 proteins are involved in the regeneration of ascorbate through transmembrane electron transport [103,104] and have previously been implicated in drought tolerance through redox homeostasis [105]. The functionally uncharacterized β sheet-rich DOMON domain has been implicated in sugar and heme recognition [106] and predicted to be involved in protein-protein interactions, putatively functioning in metabolic signaling, in redox reactions, or both. Interestingly, LOC_Os01g67030 thus has the potential to link sugar signaling and ROS signaling, both of which have emerged as essential in the DTY-IL-specific drought response.

The 5 AA differences in the N22v2 prediction of LOC_Os01g67030 sequence fall under the two conserved domains (Figure S19). Notably they include two proline conversions and a glycine deletion, with potential structural implications, particularly in the context of transmembrane domains and β sheets [103,104]. This could affect the ability of the Cyt_b561 domain to mediate transmembrane transport and the DOMON domain to mediate protein-protein interactions or ligand binding.

Efficient ROS scavenging was identified as a key mechanism of RDS tolerance in both panicles and flag-leaves of DTY-IL. In the panicle, LOC_Os01g67030 could directly contribute to ROS homeostasis and with ROS being increasingly implicated in stress signaling including modulation of gene expression [107,108], LOC_Os01g67030 activity could be responsible for the some of the expression changes observed in P-M10 and P-M15. LOC_Os01g67030, however, was not expressed in flag-leaves.

It is possible that the ultimate positive effects of the N22 allele of LOC_Os01g67030 on seed setting in DTY-IL panicles could increase sink strength in a way that it positively affects the source strength of flag-leaves, which could contribute to maintained photosynthetic rates. A similar sink on source effects has been demonstrated by manipulation of SnRK1 dependent metabolic signaling in maize under control and drought [109].

LOC_Os03g03510 was found downregulated in DTY-IL. Both CIPK_C domain [110] and SnRK3 domain [111,112] have been implicated in abiotic stress responses, including drought tolerance. In addition, SnRK3, like SnRK1 [62,109] has been demonstrated to function in metabolic signaling and source-sink relationships. In sinks, SnRK1 activity has detrimental effects on grain filling [109]. A 35 AA C-terminal extension in the N22 allele could have functional implications, which, in addition to its observed downregulation could reduce its efficiency in DTY-IL. The postulated effect would be altered downstream phosphorylation responses with potential transcriptional changes that reflect some of the differences seen between Swarna and DTY-IL Ultimately this could contribute to maintained sink strength of the panicle with putative effects on flag-leaf source metabolism.

In theory the postulated functions of both candidates could have synergistic effects that could explain a range of the observed DTY-IL specific drought responses. Gene validation studies expressing the N22 allele of LOC_Os01g67030, LOC_Os03g03510, or both, under control of their native promoters in drought susceptible *indica* background, respective knock-outs in DTY-IL, or both, are needed to confirm their postulated roles.

5. Conclusions

This study provided novel insight into global transcriptional responses in rice under moderate RDS in a DTY-dependent manner and highlighted associated physiological mechanisms that allow DTY-IL to better cope with RDS. In DTY-IL flag-leaves, structural and metabolic integrity associated with cell wall re-organization and active ROS metabolism prevent leaf rolling and allow for maintenance of cellular growth and homeostasis under RDS, which supports sustained rates of photosynthetic activity and consequently provisioning of energy and carbon to developing sinks. In the developing panicles close to anthesis, sustained energy and carbon allocation enables the minimizing of damage to reproductive structures due to RDS through protective mechanisms, including ROS homeostasis, post-transcriptional modifications, detoxification, and secondary metabolite production; ultimately this results in improved fertility and yield under moderate RDS (Figure S21). Assessment of DTY-specific allelic variation within the *qDTY1.1* and *qDTY3.2* regions prioritized two candidate genes in DTY-IL, a predicted auxin-responsive protein with a DOMON_DOH and a Cyt_*b561* domain, and a CIPK_C and SnRK3-domain-containing protein, which might positively affect source-sink regulation under drought.

Supplementary Materials: The following are available online at http://www.mdpi.com/2073-4425/11/10/1124/s1, Table S1. Mapping results of RNA-Seq reads of Swarna and DTY-IL in flag-leaf and emerging panicle tissues under RDS and control conditions, Table S2. GO enrichment analysis of the commonly down-regulated genes in DTY-IL and Swarna under RDS in the flag-leaf and emerging panicle tissues, Table S3. Pathway enrichment analysis of Swarna downregulated and DTY-IL upregulated DEGs in flag-leaf under RDS, Table S4. Overrepresented *cis*-acting elements of Swarna downregulated and DTY-IL upregulated DEGs in flag-leaf under RDS, Table S5. GO enrichment analysis of the commonly up-regulated genes in DTY-IL and Swarna under RDS in the flag-leaf and emerging panicle tissues, Table S6. Pathway enrichment analysis of Swarna downregulated and DTY-IL upregulated DEGs in emerging panicle under RDS, Table S7. Overrepresented *cis*-acting elements of Swarna downregulated and DTY-IL upregulated DEGs in emerging panicle under RDS, Table S8. List of different module color and sizes generated in flag-leaf and emerging panicle tissue using WGCNA, Table S9. The top 10 Go terms in biological process, molecular function, and cellular component categories in M1 and M2 in flag-leaf and emerging panicle tissues under RDS, Table S10. The list of 140 and 102 genes with their putative functions and expression profiles in the DTY-IL and Swarna under RDS in the M14 and M16 modules in flag-leaf tissue, Table S11. Identified hub genes in M14 and M16 in flag-leaf with their putative functions and expression profiles between the DTY-IL and Swarna under RDS, Table S12. The list of 138 and 73 with their putative functions and expression profiles in the DTY-IL and Swarna under RDS in the M10 and M15 modules in panicle tissue, Table S13. Identified hub genes in M10 and M15 in panicle with their putative functions and expression profiles between the DTY-IL and Swarna under RDS, Table S14. qRT-PCR primers used in the study, Table S15. Information on the introgressed chromosome segments and the differentially expressed genes in the DTY1.1-IL compared with

Swarna under control and reproductive-drought stress conditions and overlapping *qDTY's* in flag-leaf and panicle tissues, Table S16. List of DEGs in the *qDTY1.1* region across the different pairwise comparisons in flag-leaf and emerging panicle transcriptomes under RDS, Table S17. Distinct *cis* regulatory elements in the 2 kb upstream promoter region of LOC_Os01g67030 in Nipponbare, MH63, and N22 sequences, Figure S1. Climate data and soil water content during water stress treatment. Figure S2. Quality control assessment for 16 flag-leaf tissue samples, Figure S3. Quality control assessment for 15 panicle tissue samples, with one Swarna control outlier removed, Figure S4. Quality control assessment for 16 panicle tissue samples, Figure S5. DEGs identification, Figure S6. Venn diagrams of differentially expressed genes (DEGs), Figure S7. Flag-leaf significant GO terms of biological processes that are down-regulated in Swarna (A) and up-regulated in DTY-IL (B) under RDS, Figure S8. Panicle significant GO terms of biological processes that are down-regulated in Swarna (A) and up-regulated in DTY-IL (B) under RDS, Figure S9. Mapman overview of the DEGs of interest in DTY-IL and Swarna under RDS, Figure S10. Identification of gene co-expression modules in the flag-leaf (A-C) and panicle (D-F) transcriptome under RDS, Figure S11. Bar graphs and Heatmaps of M1 and M2 in flag-leaf and panicle tissues under RDS, Figure S12. Major biological processes and over-represented GO Slim descriptions of drought-responsive M14 (A) and M16 (B) in flag-leaf tissue under RDS, Figure S13. Hub genes from the drought-responsive modules in the flag-leaf, Figure S14. Major biological processes and over-represented GO Slim descriptions of drought responsive M10 (A) and M15 (B) in panicle tissue under RDS, Figure S15. Hub genes from the drought-responsive modules in the panicles, Figure S16. The tissue-specific expression under RDS, Figure S17. qRT-PCR validation of candidate genes, Figure S18. Gene structure including the 2 kb upstream region of LOC_Os01g67030 in the three published reference genomes representing Nipponbare, *indica*, and *ausboro*, Figure S19. Multiple peptide sequence alignment of LOC_Os01g67030 in Nipponbare, MH63, and N22 sequences, Figure S20. Multiple peptide sequence alignment of LOC_Os03g03510 in Nipponbare, MH63, and N22 sequences. Figure S21. Model of suggested DTY-IL dependent drought tolerance mechanisms.

Author Contributions: J.A.T. and T.K. conceptualized and designed the experiment; J.A.T. and S.C. performed the experiments; J.A.T. conducted the data analyses; R.M., J.D.A., and P.B. supervised on some of the data analyses; J.A.T. and T.K. wrote the manuscript; R.M. and A.K. (Ajay Kohli) contributed to reviewing and editing; S.D. gave the seeds; A.K. (Arvind Kumar) was involved in funding acquisition. All authors have read and agreed to the published version of the manuscript.

Funding: This work was supported by the Bill and Melinda Gates Foundation.

Acknowledgments: We thank the Bill and Melinda Gates Foundation for the project support.

Conflicts of Interest: The authors declare no conflict of interest and the funders had no role in the design of the study; in the collection, analyses, or interpretation of data; in the writing of the manuscript, or in the decision to publish the results.

References

1. Borah, P.; Sharma, E.; Kaur, A.; Chandel, G.; Mohapatra, T.; Kapoor, S.; Khurana, J.P. Analysis of drought-responsive signalling network in two contrasting rice cultivars using transcriptome-based approach. *Sci. Rep.* **2017**, *7*, 42131. [CrossRef] [PubMed]
2. Peng, S.; Cassman, K.G.; Virmani, S.S.; Sheehy, J.; Khush, G.S. Yield Potential Trends of Tropical Rice since the Release of IR8 and the Challenge of Increasing Rice Yield Potential. *Crop Sci.* **1999**, *39*, 1552–1559. [CrossRef]
3. Todaka, D.; Shinozaki, K.; Yamaguchi-Shinozaki, K. Recent advances in the dissection of drought-stress regulatory networks and strategies for development of drought-tolerant transgenic rice plants. *Front. Plant Sci.* **2015**, *6*, 84. [CrossRef] [PubMed]
4. Lafitte, H.R.; Price, A.H.; Courtois, B. Yield response to water deficit in an upland rice mapping population: Associations among traits and genetic markers. *Theor. Appl. Genet.* **2004**, *109*, 1237–1246. [CrossRef]
5. Venuprasad, R.; Lafitte, H.R.; Atlin, G.N. Response to Direct Selection for Grain Yield under Drought Stress in Rice. *Crop Sci.* **2007**, *47*, 285–293. [CrossRef]
6. Liu, J.; Bennett, J. Reversible and Irreversible Drought-Induced Changes in the Anther Proteome of Rice (*Oryza sativa* L.) Genotypes IR64 and Moroberekan. *Mol. Plant* **2011**, *4*, 59–69. [CrossRef]
7. Vikram, P.; Swamy, B.P.; Dixit, S.; Ahmed, H.; Cruz, M.T.; Singh, A.; Kumar, A. QDTY1.1, a major QTL for rice grain yield under reproductive-stage drought stress with a consistent effect in multiple elite genetic backgrounds. *BMC Genet.* **2011**, *12*, 89. [CrossRef]
8. Jin, Y.; Yang, H.; Wei, Z.; Ma, H.; Ge, X. Rice Male Development under Drought Stress: Phenotypic Changes and Stage-Dependent Transcriptomic Reprogramming. *Mol. Plant* **2013**, *6*, 1630–1645. [CrossRef]
9. Guo, C.; Ge, X.; Ma, H. The rice OsDIL gene plays a role in drought tolerance at vegetative and reproductive stages. *Plant Mol. Biol.* **2013**, *82*, 239–253. [CrossRef]

10. Shankar, R.; Bhattacharjee, A.; Jain, M. Transcriptome analysis in different rice cultivars provides novel insights into desiccation and salinity stress responses. *Sci. Rep.* **2016**, *6*, 23719. [CrossRef]
11. Pandey, S. Economic costs of drought and rice farmers' coping mechanisms. *Int. Rice Res. Notes* **2009**, *32*, 1. [CrossRef]
12. Kumar, A.; Dixit, S.; Ram, T.; Yadaw, R.B.; Mishra, K.K.; Mandal, N.P. Breeding high-yielding drought-tolerant rice: Genetic variations and conventional and molecular approaches. *J. Exp. Bot.* **2014**, *65*, 6265–6278. [CrossRef] [PubMed]
13. Kumar, A.; Sandhu, N.; Dixit, S.; Yadaw, S.; Swamy, M.P.; Shamsudin, N.A. Marker-assisted selection strategy to pyramid two or more QTLs for quantitative trait-grain yield under drought. *Rice* **2018**, *11*, 35. [CrossRef] [PubMed]
14. Bernier, J.; Kumar, A.; Ramaiah, V.; Spaner, D.; Atlin, G.A. Large-Effect QTL for Grain Yield under Reproductive-Stage Drought Stress in Upland Rice. *Crop Sci.* **2007**, *47*, 507. [CrossRef]
15. Venuprasad, R.; Bool, M.E.; Quiatchon, L.; Atlin, G.N. A QTL for rice grain yield in aerobic environments with large effects in three genetic backgrounds. *Theor. Appl. Genet.* **2011**, *124*, 323–332. [CrossRef]
16. Ghimire, K.H.; Quiatchon, L.A.; Vikram, P.; Swamy, B.M.; Dixit, S.; Ahmed, H.; Hernandez, J.; Borromeo, T.; Kumar, A. Identification and mapping of a QTL (qDTY1.1) with a consistent effect on grain yield under drought. *Field Crop. Res.* **2012**, *131*, 88–96. [CrossRef]
17. Yadaw, R.B.; Dixit, S.; Raman, A.; Mishra, K.K.; Vikram, P.; Swamy, B.M.; Sta Cruz, M.T.; Maturan, P.; Pandey, M.; Kumar, A. A QTL for high grain yield under lowland drought in the background of popular rice variety Sabitri from Nepal. *Field Crop. Res.* **2013**, *144*, 281–287. [CrossRef]
18. Dixit, S.; Biswal, A.K.; Min, A.; Henry, A.; Oane, R.H.; Raorane, M.L.; Longkumer, T.; Pabuayon, I.M.; Mutte, S.K.; Vardarajan, A.R.; et al. Action of multiple intra-QTL genes concerted around a co-localized transcription factor underpins a large effect QTL. *Sci. Rep.* **2015**, *5*, 15183. [CrossRef]
19. Raorane, M.L.; Pabuayon, I.M.; Varadarajan, A.R.; Mutte, S.K.; Kumar, A.; Treumann, A.; Kohli, A. Proteomic insights into the role of the large-effect QTL qDTY 12.1 for rice yield under drought. *Mol. Breed.* **2015**, *35*, 6. [CrossRef]
20. Degenkolbe, T.; Do, P.T.; Zuther, E.; Repsilber, D.; Walther, D.; Hincha, D.K.; Köhl, K.I. Expression profiling of rice cultivars differing in their tolerance to long-term drought stress. *Plant Mol. Biol.* **2009**, *69*, 133–153. [CrossRef]
21. Lenka, S.K.; Katiyar, A.; Chinnusamy, V.; Bansal, K.C. Comparative analysis of drought-responsive transcriptome in Indica rice genotypes with contrasting drought tolerance. *Plant Biotechnol. J.* **2011**, *9*, 315–327. [CrossRef] [PubMed]
22. Ray, S.; Dansana, P.K.; Giri, J.; Deveshwar, P.; Arora, R.; Agarwal, P.; Khurana, J.P.; Kapoor, S.; Tyagi, A.K. Modulation of transcription factor and metabolic pathway genes in response to water-deficit stress in rice. *Funct. Integr. Genom.* **2011**, *11*, 157–178. [CrossRef] [PubMed]
23. Wang, D.; Pan, Y.; Zhao, X.; Zhu, L.; Fu, B.; Li, Z. Genome-wide temporal-spatial gene expression profiling of drought responsiveness in rice. *BMC Genom.* **2011**, *12*, 149. [CrossRef] [PubMed]
24. Huang, L.; Zhang, F.; Zhang, F.; Wang, W.; Zhou, Y.; Fu, B.; Li, Z. Comparative transcriptome sequencing of tolerant rice introgression line and its parents in response to drought stress. *BMC Genom.* **2014**, *15*, 1–26. [CrossRef]
25. Hu, H.; Xiong, L. Genetic Engineering and Breeding of Drought-Resistant Crops. *Annu. Rev. Plant Biol.* **2014**, *65*, 715–741. [CrossRef]
26. Baldoni, E.; Bagnaresi, P.; Locatelli, F.; Mattana, M.; Genga, A. Comparative Leaf and Root Transcriptomic Analysis of two Rice Japonica Cultivars Reveals Major Differences in the Root Early Response to Osmotic Stress. *Rice* **2016**, *9*, 25. [CrossRef]
27. Zhang, Z.; Li, Y.; Xiao, B. Comparative transcriptome analysis highlights the crucial roles of photosynthetic system in drought stress adaptation in upland rice. *Sci. Rep.* **2008**, *6*, 19349. [CrossRef]
28. Arvidsson, S.; Kwasniewski, M.; Riano-Pachon, D.M.; Mueller-Roeber, B. QuantPrime-a flexible tool for reliable high-throughput primer design for quantitative PCR. *BMC Bioinform.* **2016**, *9*, 465. [CrossRef]
29. Umezawa, T.; Fujita, M.; Fujita, Y.; Yamaguchi-Shinozaki, K.; Shinozaki, K. Engineering drought tolerance in plants: Discovering and tailoring genes to unlock the future. *Curr. Opin. Biotechnol.* **2006**, *17*, 113–122. [CrossRef]

30. Moumeni, A.; Satoh, K.; Kondoh, H.; Asano, T.; Hosaka, A.; Venuprasad, R.; Serraj, R.; Kumar, A.; Leung, H.; Kikuchi, S. Comparative analysis of root transcriptome profiles of two pairs of drought-tolerant and susceptible rice near-isogenic lines under different drought stress. *BMC Plant Biol.* **2011**, *11*, 174. [CrossRef]
31. Ding, X.; Li, X.; Xiong, L. Insight into Differential Responses of Upland and Paddy Rice to Drought Stress by Comparative Expression Profiling Analysis. *Int. J. Mol. Sci.* **2013**, *14*, 5214–5238. [CrossRef]
32. Weng, X.; Wang, L.; Wang, J.; Hu, Y.; Du, H.; Xu, C.; Xing, Y.; Li, X.; Xiao, J.; Zhang, Q. Grain Number, Plant Height, and Heading Date7 Is a Central Regulator of Growth, Development, and Stress Response. *Plant Physiol.* **2014**, *164*, 735–747. [CrossRef]
33. Moumeni, A.; Satoh, K.; Venuprasad, R.; Serraj, R.; Kumar, A.; Leung, H.; Kikuchi, S. Transcriptional profiling of the leaves of near-isogenic rice lines with contrasting drought tolerance at the reproductive stage in response to water deficit. *BMC Genom.* **2015**, *16*, 1110. [CrossRef] [PubMed]
34. Wei, H.; Chen, C.; Ma, X.; Zhang, Y.; Han, J.; Mei, H.; Yu, S. Comparative Analysis of Expression Profiles of Panicle Development among Tolerant and Sensitive Rice in Response to Drought Stress. *Front. Plant Sci.* **2017**, *8*, 437. [CrossRef] [PubMed]
35. Hadiarto, T.; Tran, L.P. Progress studies of drought-responsive genes in rice. *Plant Cell Rep.* **2010**, *30*, 297–310. [CrossRef] [PubMed]
36. Shojaie, A.; Michailidis, G. Analysis of Gene Sets Based on the Underlying Regulatory Network. *J. Comput. Biol.* **2009**, *16*, 407–426. [CrossRef] [PubMed]
37. Dela Fuente, A. From 'differential expression' to 'differential networking'–identification of dysfunctional regulatory networks in diseases. *Trends Genet.* **2010**, *26*, 326–333. [CrossRef] [PubMed]
38. Gitter, A.; Carmi, M.; Barkai, N.; Bar-Joseph, Z. Linking the signaling cascades and dynamic regulatory networks controlling stress responses. *Genome Res.* **2013**, *23*, 365–376. [CrossRef] [PubMed]
39. Ma, C.; Xin, M.; Feldmann, K.A.; Wang, X. Machine Learning-Based Differential Network Analysis: A Study of Stress-Responsive Transcriptomes in Arabidopsis. *Plant Cell* **2014**, *26*, 520–537. [CrossRef]
40. Zhang, B.; Horvath, S. A General Framework for Weighted Gene Co-Expression Network Analysis. Stat. Appl. Genet. *Mol. Biol.* **2005**, *4*, 17.
41. Gehan, M.A.; Greenham, K.; Mockler, T.C.; Mcclung, C.R. Transcriptional networks—crops, clocks, and abiotic stress. *Curr. Opin. Plant Biol.* **2015**, *24*, 39–46. [CrossRef] [PubMed]
42. Liseron-Monfils, C.; Ware, D. Revealing gene regulation and associations through biological networks. *Curr. Plant Biol.* **2015**, *3–4*, 30–39. [CrossRef]
43. Segal, E.; Shapira, M.; Regev, A.; Peer, D.; Botstein, D.; Koller, D.; Friedman, N. Module networks: Identifying regulatory modules and their condition-specific regulators from gene expression data. *Nat. Genet.* **2003**, *34*, 166–176. [CrossRef] [PubMed]
44. Sircar, S.; Parekh, N. Functional characterization of drought-responsive modules and genes in Oryza sativa: A network-based approach. *Front. Genet.* **2015**, *6*, 256. [CrossRef] [PubMed]
45. Horvath, S.; Dong, J. Geometric Interpretation of Gene Coexpression Network Analysis. *PLoS Comput. Biol.* **2008**, *4*, 1–27. [CrossRef]
46. Langfelder, P.; Horvath, S. WGCNA: An R package for weighted correlation network analysis. *BMC Bioinform.* **2008**, *9*, 559. [CrossRef]
47. Shaik, R.; Ramakrishna, W. Genes and Co-Expression Modules Common to Drought and Bacterial Stress Responses in Arabidopsis and Rice. *PLoS ONE* **2013**, *8*, 10. [CrossRef]
48. Zhang, L.; Yu, S.; Zuo, K.; Luo, L.; Tang, K. Identification of Gene Modules Associated with Drought Response in Rice by Network-Based Analysis. *PLoS ONE* **2012**, *7*, 5. [CrossRef]
49. Counce, P.A.; Keisling, T.C.; Mitchell, A. A Uniform, Objective, and Adaptive System for Expressing Rice Development. *Crop Sci.* **2000**, *40*, 436. [CrossRef]
50. Krishnan, A.; Gupta, C.; Ambavaram, M.M.R.; Pereira, A. RECoN: Rice Environment Coexpression Network for Systems Level Analysis of Abiotic-Stress Response. *Front. Plant Sci.* **2017**, *8*, 1–15. [CrossRef]
51. Andrews, S. FastQC: A Quality Control Tool for High Throughput Sequence Data. 2010. Available online: http://www.bioinformatics.babraham.ac.uk/projects/fastqc/ (accessed on 23 September 2020).
52. Bolger, A.M.; Lohse, M.; Usadel, B. Trimmomatic: A flexible trimmer for Illumina sequence data. *Bioinformatics* **2014**, *30*, 2114–2120. [CrossRef] [PubMed]

53. Trapnell, C.; Williams, B.; Pertea, G. Transcript assembly and quantification by RNA-Seq reveals unannotated transcripts and isoform switching during cell differentiation. *Nat. Biotechnol.* **2010**, *28*, 511–515. [CrossRef] [PubMed]
54. Patro, R.; Duggal, G.; Love, M.I.; Irizarry, R.A.; Kingsford, C. Salmon provides fast and bias-aware quantification of transcript expression. *Nat. Methods* **2017**, *14*, 417–419. [CrossRef] [PubMed]
55. Soneson, C.; Love, M.I.; Robinson, M.D. Differential analyses for RNA-seq: Transcript-level estimates improve gene-level inferences. *F1000 Res.* **2016**, *4*, 1521. [CrossRef]
56. Love, M.I.; Huber, W.; Anders, S. Moderated estimation of fold change and dispersion for RNA-seq data with DESeq2. *Genome Biol.* **2014**, *15*, 550. [CrossRef]
57. Livak, K.J.; Schmittgen, T.D. Analysis of relative gene expression data using real-time quantitative PCR and the $2^{-\Delta\Delta C}{}_{T}$ method. *Methods* **2001**, *25*, 402–408. [CrossRef]
58. Morales, K.Y.; Singh, N.; Perez, F.A.; Ignacio, J.C.; Thapa, R.; Arbelaez, J.D.; Tabien, R.E.; Famoso, A.; Wang, D.R.; Septiningsih, E.M.; et al. An improved 7K SNP array, the C7AIR, provides a wealth of validated SNP markers for rice breeding and genetics studies. *PLoS ONE* **2020**, *15*, e0232479. [CrossRef]
59. Vikram, P.; Swamy, B.P.; Dixit, S.; Singh, R.; Singh, B.P.; Miro, B.; Kohli, A.; Henry, A.; Singh, N.K.; Kumar, A. Drought susceptibility of modern rice varieties: An effect of linkage of drought tolerance with undesirable traits. *Sci. Rep.* **2015**, *5*, 14799. [CrossRef]
60. Hirota, O.; Oka, M.; Takeda, T. Sink Activity Estimation by Sink Size and Dry Matter Increase During the Ripening Stage of Barley (*Hordeum vulgare*) and Rice (*Oryza sativa*). *Ann. Bot.* **1990**, *65*, 349–353. [CrossRef]
61. Biswal, A.K.; Kohli, A. Cereal flag leaf adaptations for grain yield under drought: Knowledge status and gaps. *Mol. Breed.* **2013**, *31*, 749–766. [CrossRef]
62. Lawlor, D.W.; Paul, M.J. Source/sink interactions underpin crop yield: The case for trehalose 6-phosphate/SnRK1 in improvement of wheat. *Front. Plant Sci.* **2014**, *5*, 418. [CrossRef] [PubMed]
63. Basu, S.; Ramegowda, V.; Kumar, A.; Pereira, A. Plant adaptation to drought stress. *F1000 Res.* **2016**, *5*, 1554. [CrossRef] [PubMed]
64. Guo, C.; Yao, L.; You, C.; Wang, S.; Cui, J.; Ge, X.; Ma, H. MID1 plays an important role in response to drought stress during reproductive development. *Plant J.* **2016**, *88*, 280–293. [CrossRef] [PubMed]
65. Farooq, M.; Wahid, A.; Kobayashi, N.; Fujita, D.; Basra, S.M. Plant Drought Stress: Effects, Mechanisms and Management. *Sustain. Agric.* **2009**, *29*, 153–188.
66. Moore, J.P.; Vicré-Gibouin, M.; Farrant, J.M.; Driouich, A. Adaptations of higher plant cell walls to water loss: Drought vs. desiccation. *Physiol. Plant.* **2008**, *134*, 237–245. [CrossRef]
67. Tenhaken, R. Cell wall remodeling under abiotic stress. *Front. Plant Sci.* **2015**, *5*, 771. [CrossRef]
68. Cal, A.; Sanciangco, M.; Rebolledo, M.B.; Luquet, D.; Torres, R.; McnNaly, K.; Henry, A. Leaf morphology, rather than plant water status, underlies, genetic variation of rice leaf rolling under drought. *Plant Cell Environ.* **2019**, *42*, 1532–1544. [CrossRef]
69. Szklarczyk, D.; Morris, J.H.; Cook, H.; Kuhn, M.; Wyder, S.; Simonovic, M.; Santos, A.; Doncheva, N.T.; Roth, A.; Bork, P.; et al. The STRING database in 2017: Quality-controlled protein–protein association networks, made broadly accessible. *Nucleic Acids Res.* **2017**, *45*, D362–D368. [CrossRef]
70. Cosgrove, D.J. Growth of the plant cell wall. *Nat. Rev. Mol. Cell Biol.* **2005**, *6*, 850–861. [CrossRef]
71. Wu, Y.; Sharp, R.E.; Durachko, D.M.; Cosgrove, D.J. Growth Maintenance of the Maize Primary Root at Low Water Potentials Involves Increases in Cell-Wall Extension Properties, Expansin Activity, and Wall Susceptibility to Expansins. *Plant Physiol.* **1996**, *111*, 765–772. [CrossRef]
72. Jones, L.; Mcqueen-Mason, S. A role for expansins in dehydration and rehydration of the resurrection plantCraterostigma plantagineum. *FEBS Lett.* **2004**, *559*, 61–65. [CrossRef]
73. Harb, A.; Krishnan, A.; Ambavaram, M.M.; Pereira, A. Molecular and Physiological Analysis of Drought Stress in Arabidopsis Reveals Early Responses Leading to Acclimation in Plant Growth. *Plant Physiol.* **2010**, *154*, 1254–1271. [CrossRef] [PubMed]
74. Guo, W.; Zhao, J.; Li, X.; Qin, L.; Yan, X.; Liao, H. A soybean β-expansin gene GmEXPB2 intrinsically involved in root system architecture responses to abiotic stresses. *Plant J.* **2011**, *66*, 541–552. [CrossRef] [PubMed]
75. Li, F.; Han, Y.; Feng, Y.; Xing, S.; Zhao, M.; Chen, Y.; Wang, W. Expression of wheat expansin driven by the RD29 promoter in tobacco confers water-stress tolerance without impacting growth and development. *J. Biotechnol.* **2013**, *163*, 281–291. [CrossRef]

76. Dai, F.; Zhang, C.; Jiang, X.; Kang, M.; Yin, X.; Lu, P.; Zhang, X.; Zheng, Y.; Gao, J. RhNAC2 and RhEXPA4 Are Involved in the Regulation of Dehydration Tolerance during the Expansion of Rose Petals. *Plant Physiol.* **2012**, *160*, 2064–2082. [CrossRef]
77. Torres, M.A.; Dangl, J.L. Functions of the respiratory burst oxidase in biotic interactions, abiotic stress and development. *Curr. Opin. Plant Biol.* **2005**, *8*, 397–403. [CrossRef]
78. Shigeto, J.; Tsutsumi, Y. Diverse functions and reactions of class III peroxidases. *New Phytol.* **2016**, *209*, 1395–1402. [CrossRef]
79. Raggi, S.; Ferrarini, A.; Delledonne, M.; Dunand, C.; Ranocha, P.; Lorenzo, G.D.; Cervone, F.; Ferrari, S. The Arabidopsis thaliana Class III Peroxidase AtPRX71 Negatively Regulates Growth under Physiological Conditions and in Response to Cell Wall Damage. *Plant Physiol.* **2015**, *169*, 2513–2525. [CrossRef]
80. Passardi, F.; Penel, C.; Dunand, C. Performing the paradoxical: How plant peroxidases modify the cell wall. *Trends Plant Sci.* **2004**, *9*, 534–540. [CrossRef]
81. Kunieda, T.; Shimada, T.; Kondo, M.; Nishimura, M.; Nishitani, K.; Hara-Nishimura, I. Spatiotemporal Secretion of PEROXIDASE36 Is Required for Seed Coat Mucilage Extrusion in Arabidopsis. *Plant Cell* **2013**, *25*, 1355–1367. [CrossRef]
82. Miller, G.; Suzuki, N.; Ciftci-Yilmaz, S.; Mittler, R. Reactive oxygen species homeostasis and signalling during drought and salinity stresses. *Plant Cell Environ.* **2010**, *33*, 453–467. [CrossRef]
83. You, J.; Chan, Z. ROS Regulation During Abiotic Stress Responses in Crop Plants. *Front. Plant Sci.* **2015**, *6*, 1092. [CrossRef] [PubMed]
84. Patro, L.; Mohapatra, P.K.; Biswal, U.C.; Biswal, B. Dehydration induced loss of photosynthesis in Arabidopsis leaves during senescence is accompanied by the reversible enhancement in the activity of cell wall β-glucosidase. *J. Photochem. Photobiol. B Biol.* **2014**, *137*, 49–54. [CrossRef] [PubMed]
85. Wang, X.; Cai, X.; Xu, C.; Wang, Q.; Dai, S. Drought-Responsive Mechanisms in Plant Leaves Revealed by Proteomics. *Int. J. Mol. Sci.* **2016**, *17*, 1706. [CrossRef] [PubMed]
86. Voss, I.; Sunil, B.; Scheibe, R.; Raghavendra, A.S. Emerging concept for the role of photorespiration as an important part of abiotic stress response. *Plant Biol.* **2013**, *15*, 713–722. [CrossRef] [PubMed]
87. Noctor, G.; Mhamdi, A.; Foyer, C.H. The Roles of Reactive Oxygen Metabolism in Drought: Not So Cut and Dried. *Plant Physiol.* **2014**, *164*, 1636–1648. [CrossRef]
88. Nakabayashi, R.; Yonekura-Sakakibara, K.; Urano, K.; Suzuki, M.; Yamada, Y.; Nishizawa, T.; Matsuda, F.; Kojima, F.; Sakakibara, H.; Shinozaki, K.; et al. Enhancement of oxidative and drought tolerance in Arabidopsis by overaccumulation of antioxidant flavonoids. *Plant J.* **2014**, *77*, 367–379. [CrossRef]
89. Wang, J.; Lan, P.; Gao, H.; Zheng, L.; Li, W.; Schmidt, W. Expression changes of ribosomal proteins in phosphate-and iron-deficient Arabidopsis roots predict stress-specific alterations in ribosome composition. *BMC Genom.* **2013**, *14*, 783. [CrossRef]
90. Miazek, A.; Zagdańska, B. Involvement of exopeptidases in dehydration tolerance of spring wheat seedlings. *Biologia Plant.* **2008**, *52*, 687–694. [CrossRef]
91. Zhang, Z.; Zhang, Q.; Wu, J.; Zheng, X.; Zheng, S.; Sun, X.; Qiu, Q.; Lu, T. Gene Knockout Study Reveals That Cytosolic Ascorbate Peroxidase 2(OsAPX2) Plays a Critical Role in Growth and Reproduction in Rice under Drought, Salt and Cold Stresses. *PLoS ONE* **2013**, *8*, 2. [CrossRef]
92. Cramer, G.R.; Van Sluyter, S.C.; Hopper, D.W.; Pascovici, D.; Keighley, T.; Haynes, P.A. Proteomic analysis indicates massive changes in metabolism prior to the inhibition of growth and photosynthesis of grapevine (*Vitis vinifera* L.) in response to water deficit. *BMC Plant Biol.* **2013**, *13*, 49. [CrossRef]
93. Xu, J.; Xing, X.; Tian, Y.; Peng, R.; Xue, Y.; Zhao, W.; Yao, Q. Transgenic Arabidopsis Plants Expressing Tomato Glutathione S-Transferase Showed Enhanced Resistance to Salt and Drought Stress. *PLoS ONE* **2015**, *10*, 9. [CrossRef] [PubMed]
94. Islam, T.; Manna, M.; Reddy, M.K. Glutathione Peroxidase of Pennisetum glaucum (PgGPx) Is a Functional Cd2 Dependent Peroxiredoxin that Enhances Tolerance against Salinity and Drought Stress. *PLoS ONE* **2015**, *10*, 1–18. [CrossRef] [PubMed]
95. Su, Z.; Ma, X.; Guo, H.; Sukiran, N.L.; Guo, B.; Assmann, S.M.; Ma, H. Flower Development under Drought Stress: Morphological and Transcriptomic Analyses Reveal Acute Responses and Long-Term Acclimation in Arabidopsis. *Plant Cell* **2013**, *25*, 3785–3807. [CrossRef] [PubMed]
96. Bhaskara, G.B.; Nguyen, T.T.; Verslues, P.E. Unique Drought Resistance Functions of the Highly ABA-Induced Clade A Protein Phosphatase 2Cs. *Plant Physiol.* **2012**, *160*, 379–395. [CrossRef] [PubMed]

97. Gosti, F. ABI1 Protein Phosphatase 2C Is a Negative Regulator of Abscisic Acid Signaling. *Plant Cell Online* **1999**, *11*, 1897–1910. [CrossRef] [PubMed]
98. Mandava, N.B. Plant Growth-Promoting Brassinosteroids. *Annu. Rev. Plant Physiol. Plant Mol. Biol.* **1988**, *39*, 23–52. [CrossRef]
99. Neff, M.M.; Nguyen, S.M.; Malancharuvil, E.J.; Fujioka, S.; Noguchi, T.; Seto, H.; Tsukubi, M.; Takatsuto, S.; Yoshida, S.; Chory, J. BAS1: A gene regulating brassinosteroid levels and light responsiveness in Arabidopsis. *Proc. Natl. Acad. Sci. USA* **1999**, *96*, 15316–15323. [CrossRef] [PubMed]
100. Belkhadir, Y.; Chory, J. Brassinosteroid Signaling: A Paradigm for Steroid Hormone Signaling from the Cell Surface. *Science* **2006**, *314*, 1410–1411. [CrossRef] [PubMed]
101. Clouse, S.D. Brassinosteroid Signal Transduction: From Receptor Kinase Activation to Transcriptional Networks Regulating Plant Development. *Plant Cell* **2011**, *23*, 1219–1230. [CrossRef] [PubMed]
102. Uga, Y.; Sugimoto, K.; Ogawa, S.; Rane, J.; Ishitani, M.; Hara, N.; Kitomi, Y.; Inukai, Y.; Ono, K.; Kanno, N.; et al. Control of root system architecture by DEEPER ROOTING 1 increases rice yield under drought conditions. *Nat. Genet.* **2013**, *45*, 1097–1102. [CrossRef]
103. Verelst, W.; Asard, H. A phylogenetic study of cytochrome b561 proteins. *Genome Biol.* **2003**, *4*, 6. [CrossRef] [PubMed]
104. Asard, H.; Barbaro, R.; Trost, P.; Bérczi, A. Cytochromes b561: Ascorbate-mediated trans-membrane electron transport. *Antioxid. Redox Signal.* **2013**, *19*, 1026–1035. [CrossRef] [PubMed]
105. Nanasato, Y.; Akashi, K.; Yokota, A. Co-expression of Cytochrome b561 and Ascorbate Oxidase in Leaves of Wild Watermelon under Drought and High Light Conditions. *Plant Cell Physiol.* **2005**, *46*, 1515–1524. [CrossRef]
106. Lyer, L.M.; Anantharaman, V.; Aravind, L. The DOMON domains are involved in heme and sugar recognition. *Bioinformatics* **2007**, *23*, 2660–2664.
107. Choudhury, F.K.; Rivero, R.M.; Blumwald, E.; Mittler, R. Reactive oxygen species, abiotic stress and stress combination. *Plant J.* **2016**, *90*, 856–867. [CrossRef] [PubMed]
108. Mittler, R. ROS Are Good. *Trends Plant. Sci.* **2017**, *22*, 11–19. [CrossRef]
109. Oszvald, M.; Primavesi, L.F.; Griffiths, C.A.; Cohn, J.; Basu, S.S.; Nuccio, M.L.; Paul, M.J. Trehalose 6-Phosphate Regulates Photosynthesis and Assimilate Partitioning in Reproductive Tissue. *Plant Physiol.* **2018**, *176*, 2623–2638. [CrossRef]
110. Sánchez-Barrena, M.J.; Fujii, H.; Angulo, I.; Martínez-Ripoll, M.; Zhu, J.; Albert, A. The Structure of the C-terminal Domain of the Protein Kinase AtSOS2 Bound to the Calcium Sensor AtSOS3. *Mol. Cell* **2007**, *26*, 427–435. [CrossRef]
111. Hirabak, E.M.; Chan, C.W.; Gribskov, M.; Harper, J.F.; Choi, J.H.; Halford, N.; Kudla, J.; Luan, S.; Nimmo, H.G.; Sussman, M.R.; et al. The Arabidopsis CDPK-SnRK Superfamily of Protein Kinases. *Plant Physiol.* **2003**, *132*, 666–680. [CrossRef]
112. Wang, Y.; Yan, H.; Qiu, Z.; Hu, B.; Zeng, B.; Zhong, C.; Fan, C. Comprehensive Analysis of SnRK Gene Family and their Responses to Salt Stress in Eucalyptus grandis. *Int. J. Mol. Sci.* **2019**, *20*, 2786. [CrossRef] [PubMed]